APENDIX A

The Role of Mass Transfer in Coal Gasification Processes: A Review

1.0 Introduction

This review is divided into separate sections that deal with mass transfer during devolatilization and during gasification (or combustion). This quarterly report is devoted to the first topic. This division is somewhat artificial, since normally the two processes tend to merge with one another, and it is difficult to say when devolatilization ends and gasification begins. Still, the phenomena are more easily presented in terms of the separate regimes in which they occur, and as is the sequence in nature, the material concerning devolatilization precedes that concerning gasification.

2.0 The Role Of Mass Transfer in Coal Devolatilization

The major focus of this review is "rapid rate" pyrolysis or devolatilization, involving heating of finely ground coals (of diameter of millimeters or less) at heating rates above roughly 1000 K/s to high temperatures (above 700 K). This covers all conditions of relevance in pulverized coal combustion, fluidized bed combustion or gasification, entrained flow gasification or liquefaction, and dust explosions. Much of the material presented here has been presented previously in an extensive review on mass transfer processes in coal pyrolysis (1).

The coal pyrolysis literature has been reviewed many times; within the last few years, three reasonably comprehensive reviews emphasizing rapid rate coal pyrolysis phenomena have appeared (2-4). An extensive review of the pyrolysis literature will not be presented here. Rather, the focus will be narrowed to the role of mass transfer in pyrolysis processes. This aspect of rapid rate pyrolysis processes has, until recent years, received relatively little attention. As will be discussed below, a proper understanding of mass transfer processes is central to gaining a fundamental understanding of the rapid rate pyrolysis processes.

There is abundant evidence that mass transfer processes play a role in determining the yields of volatiles obtained during pyrolysis (2-8). The majority of the evidence comes from studies in which the effect of pressure in the gas phase external to the particle is examined. Figure 1 presents a summary of data obtained with a Pittsburgh No. 8 bituminous coal. It shows clearly that as gas pressure external to a particle is increased, the yield of tar obtained during pyrolysis is decreased. At the same time, the yield of light gases increases with increasing pressure. The effect of pressure on lignite pyrolysis behavior is not nearly as significant, but is qualitatively similar (9). This point is illustrated in Fig. 2 which shows data on pressure effects for a variety of coals.

Tars have been singled out as key species in considering the effect of mass transfer limitations on coal pyrolysis. Tars are operationally defined as any room temperature condensable volatiles. Roughly one quarter to one third of both the mass (3,5,10) and heating values (6) of bituminous coals can be carried into the vapor phase by escaping tars. Up to three quarters of the total heating value of the volatiles can be contained in these tars. Tars have also been suggested as important intermediates in soot formation processes. The recent observations of soot trails around individual coal particles (inside gas flames) has been offered as evidence of tar condensation mechanisms for soot formation (11,12). It is significant that only coals which yield large quantities of tar exhibit this behavior (11). Neither the mechanisms of escape of the tar from the particles nor the mechanism of condensation of the soot is understood.

The role of mass transfer limitations in shaping yields from pyrolysis seems to be greatest in the case of bituminous coals and less so in other ranks (2-4,13). This is apparently related to the higher yields of tar produced during pyrolysis of bituminous coals, compared to other ranks. This is consistent with the observation

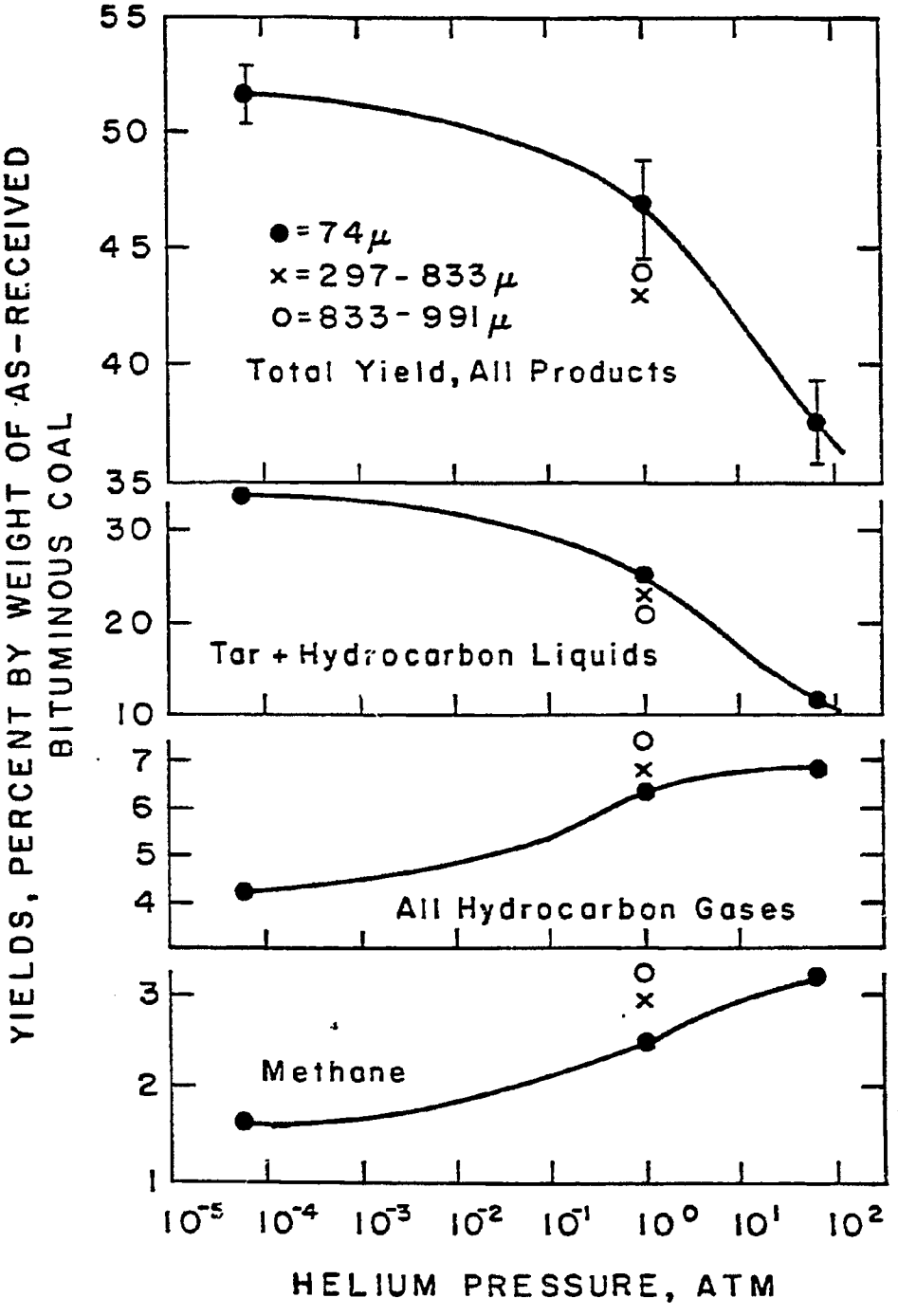

Figure 1: Effects of pressure and coal particle size on yields of total volatiles, tar, total hydrocarbon gases, and methane, from Pittsburgh Seam bituminous coal pyrolysis. Experiments performed in a heated wire mesh reactor at a heating rate of roughly 1000 K/sec. Maximum temperatures approximately 1300K, with isothermal holding periods of 2 to 10 sec. Volatile products very quickly quenched upon leaving particles, by contact with cold ambient gas or reactor walls.[5]

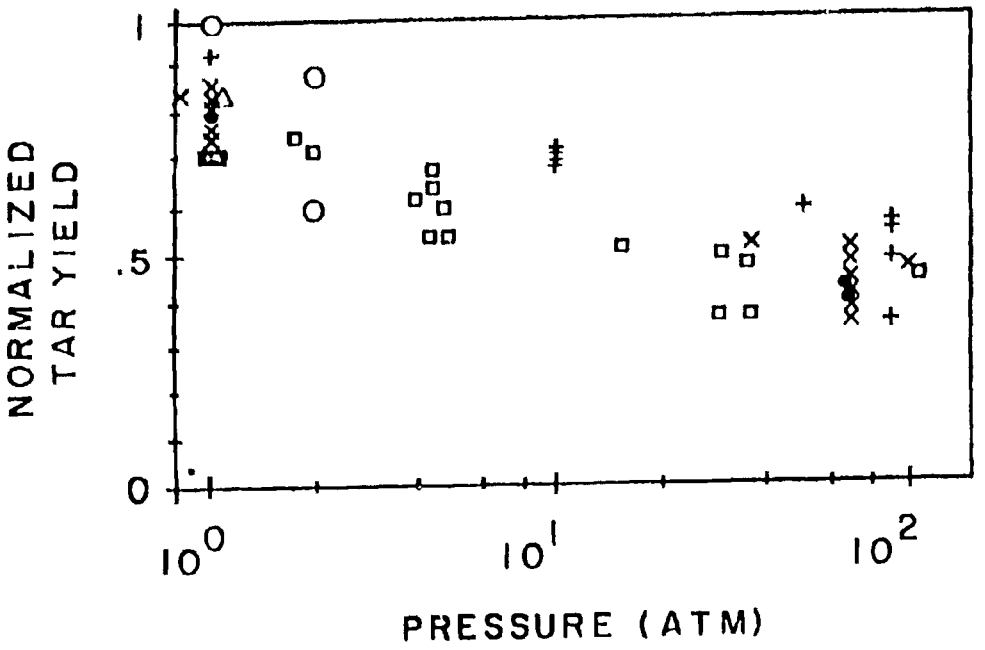

Figure 2: Variation of normalized tar yield with pressure of inert gas external to the particle during pyrolysis. See Table 1 for key to symbols, and text for basis of normalization.[1]

that the bituminous ranks tend to show more tendency towards soot trail formation than do lower ranks (11,12).

Thus Fig. 2 presents an attempt at summarizing the majority of data concerning pressure effects on yields during rapid high-temperature pyrolysis. It is nominally a plot of normalized tar yield against the pressure external to the particle during pyrolysis (all results obtained in inert gas environments). Table I summarizes the conditions under which the data in Fig. 2 were obtained. Where actual tar yield data were available, the tar yield at any pressure was normalized by dividing by the maximum tar yield obtained from the coal at vacuum conditions (see Table I for what constituted vacuum conditions in each case). Where actual measurements of tar yields were not available, estimates were made, based on correlation between normalized tar yield and weight loss (derived from all available tar yield data). This correlation was of form:

$$\text{Normalized Tar Yield} = 1-0.55((v_0-v)/(v_0-v_h)) \qquad (1)$$

where v_0 is the weight loss at the lowest pressure employed in the study, v_h is the weight loss at the highest pressure employed in the study, and v is the actual weight loss at the pressure of interest. In the case in which it was necessary to use this correlation, there was relatively little ambiguity regarding appropriate values of v_0 and v_h.

Given the admittedly crude nature of the plot a rather consistent trend of decreasing tar yield with increasing pressure is observed, regardless of the rank of coal. Note that the data include both softening and non-softening coals, ranging from the lignites to low volatile bituminous in rank. It is noteworthy also that the points which seem to fall above the general trend line were normalized with respect to 0.1 atm tar data. Many data (14,17) seem to imply that 0.1 atm is a sufficiently high pressure such that further decrease in pressure would result in further increase in yield; thus the normalization factor applied in the case of studies with minimum vacuum pressures of 0.1 atm might be too high. In any event, the data shown in Fig. 2 only suggest that there might be some common behavior patterns in all ranks of coal, obviously more data are needed to prove the point.

There is general qualitative agreement on the role of mass transfer limitations in coal pyrolysis. If the rate of escape of the tar decreases with increasing pressure, this implies a longer residence time for tar precursors in the particle, thus allowing a larger fraction of them to be repolymerized into the char structure. Once reincorporated into the solid matrix by more stable bonds, the tar precursors can yield volatiles only by reactions which involve cracking off of small side groups (hence the increased yields of gas with decreasing tar yield). The mechanism by which the increased pressure serves to retard the escape of tars from the particle is still open to some debate. The various models which have been advanced to explain this effect are outlined below.

It is customary to explore for some types of mass transfer limitations by experiments in which the diameter of particles is varied. Unfortunately, data on the variation of pyrolysis product yields with particle diameter are often influenced by unintentional variations in heat transfer conditions (18). In addition, even in situations in which heat transfer to particles is relatively well-defined, there are sometimes particle size characterization difficulties, since particles can swell and/or flow on the surface of solid supports they are in contact with. Care must also be taken to avoid maceral segregation effects in such particle size effect studies. It is well known that different macerals have differing mechanical properties, so grinding and sifting operations may lead to enrichment of certain macerals in certain size fractions (19). Since different

TABLE I (1)

Conditions for Figure 2

Reference	Symbol	Coals+	Particle Size (μm)	Heating Rate/Max. Temp.	Pressure atm.	Method
Arendt & van Heek (14)		HVB (26), HVB (25), MVB (17), LVB (9)	200-315	200°C/s 1000°C	0.1-90	HWM
Gavalas & Wilks (13)		HVB (19), SUBB (6)	110	600°C/s 500°C	0.1-2	HWM
Suuberg et al. (5,6,9)		Lignite (8) HVB (36)	53-88	1000°C/s 900°C	10^{-4}-69	HWM
Unger & Suuberg (7,24)		HVB (36)	62-88	1000°C/s 900°C	10^{-1}-1	HWM
Howard (16)		HVB (20)	400-800	1°C/s 525°C	10^{-1}-1	RETORT
*Anthony et al. (17)		HVB	70	650°C/s 1000°C	10^{-3}-69	HWM
*Niksa (8)		HVB	125	1000°C/s 750°C	10^{-4}-100	HWM

*Tar Yield

+Maximum observed tar yeilds under vacuum shown in parentheses

HWM = Heated Wire Mesh

macerals can have widely varying pyrolysis behavior (20), mass transfer issues may be clouded by chemical differences.

Nevertheless, there do exist a limited number of data on the effect of particle diameter on yields and compositions of volatiles (3-5,8). Generally, lower total volatile yields and lower tar yields are observed with increasing particle size. This is evident from the data in Figures 1 and 3. This has usually been considered as consistent with the view that longer volatiles residence times lead to lower tar yields; as will be discussed below, large particle sizes will most likely lead to longer volatiles residence times.

3.0 External Mass Transfer Limitations

Throughout this review, it will be assumed that the coal particles are motionless with respect to the surrounding gas. This viewpoint is not as restrictive as it may initially appear. In many real situations, particles as small as those of interest here (less than a millimeter in diameter) will be carried along with the gas flow at roughly the same velocity. Where this assumption is not appropriate, allowance for gas-solid slip and resultant mass transfer enhancement will be possible by techniques discussed below.

There are two main mechanisms of transport of volatile species to be considered here. Upon leaving the surface of the particle, species may diffuse away from the particle or be carried away in a convective flow. It should be recalled that the main species of interest with respect to mass transfer effects during pyrolysis are the tars; of course many light gas species are simultaneously escaping the particle. It will be assumed that once a light (non-condensable) species is formed, it can undergo no further reactions, and thus the rate of transport of these species is unimportant (except as it influences tar transport). This assumption can be challenged on the basis that light gas species can certainly undergo secondary reactions before escaping the coal particle, but to address issues of this kind would divert attention from considering the role of the obviously key component, the tars.

When attention is thus focused on the escape of tars from the surface of a coal particle, analogy with the evaporation of liquid droplets is clear. The tars are a condensed phase within the coal particle, and must evaporate and diffuse away from the surface in order to be collected as a separate condensed phase product. The similarity of the infrared spectra of tars to parent coals has long been noted (20-23), and on this basis, it has been postulated that tars are merely "depolymerization" fragments of parent coals. Since the tars are relatively high molecular weight substances, as is shown below, they are only marginally volatile, even at pyrolysis temperatures. Recent experiments with nitric oxide free radical scavengers have again suggested that the tars actually directly evolve as high molecular weight substances, rather than being formed by secondary radical recombinations in the gas phase surrounding the particles (24).

The analogy between liquid droplet evaporation and tar escape during pyrolysis has thus been explored (6,25). The theory for single component droplet evaporation is well developed and is widely employed in the combustion field (e.g. Ref. 26). The theory for multi-component droplet behavior (more like the situation that exists in coal particles) is somewhat less developed and has recently received a great deal of attention (e.g. Refs. 27-29). In essence, all droplet evaporation theories postulate that the escape of a species from the surface of a droplet is controlled by a combined vaporization and diffusional process. Vapor-liquid equilibrium is assumed to exist at the droplet surface, meaning that the concentration of tar in the vapor phase right at the particle surface is determined by the vapor pressure of the tar. The rate at which liquid (or tar) can evaporate is limited by the

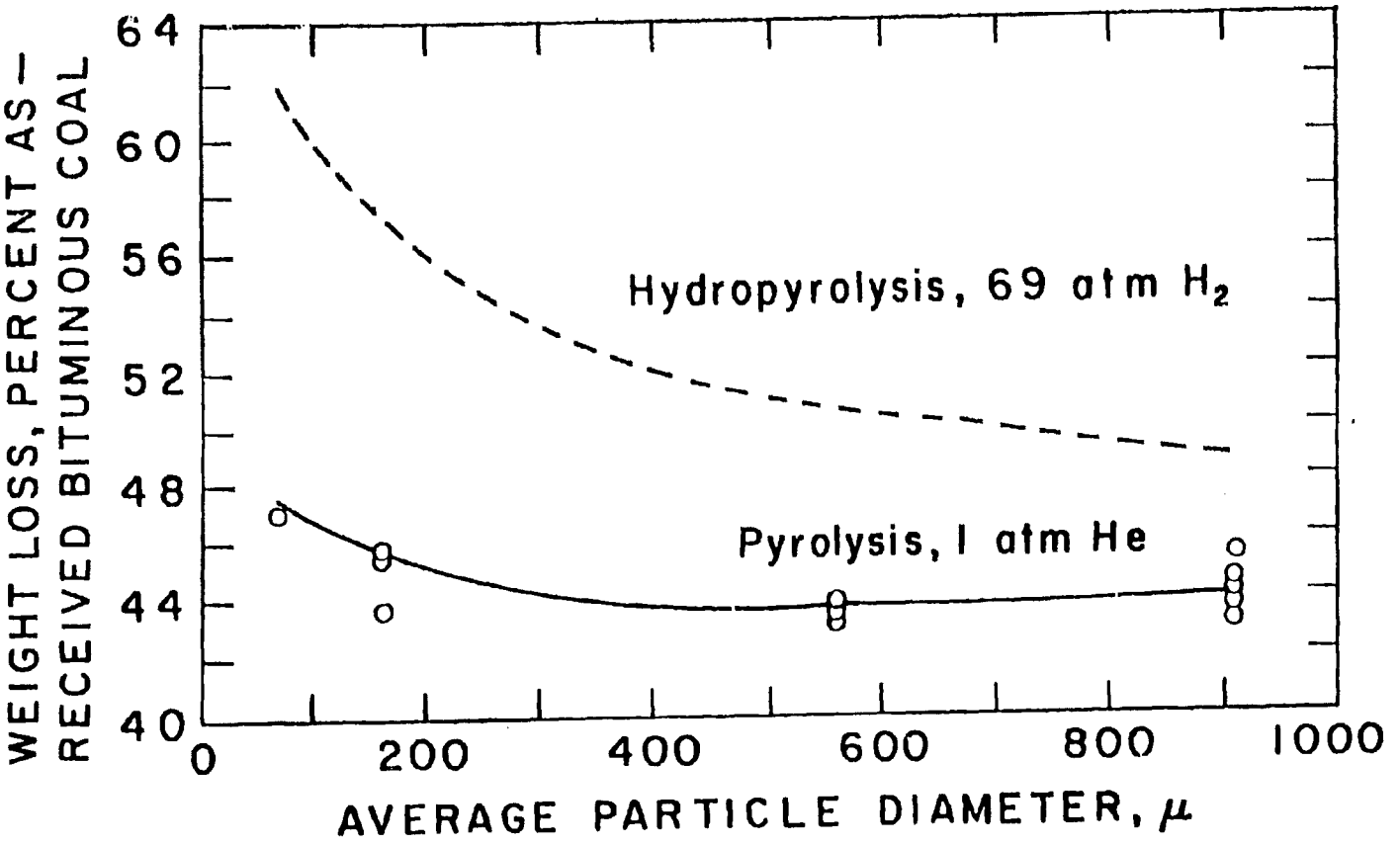

Figure 3: Effect of particle diameter on total yields from pyrolysis of a Pittsburgh Seam bituminous coal. All experiments performed in a heated wire mesh reactor at heating rates of approximately 1000 K/sec, to temperatures in excess of 820K. Isothermal holding periods of 2 to 30 sec. Particle diameter refers to original diameter; coal softens during pyrolysis. The much larger effect of particle diameter on hydropyrolysis (wherein gaseous hydrogen must diffuse into the particle) suggests the possibility of significant internal transport limitations; see Fuel, 59, 405 (1980).

requirement that this equilibrium be maintained at all times. The actual escape of the liquid or tar involves diffusion of the evaporated species through the stagnant gas surrounding the particle. The standard derivation of the model assumes a spherical droplet, but other geometries can of course be considered at the expense of greater mathematical complication. The formal mathematical statement of the model, in a form relevant for coal pyrolysis, will be presented below. If the droplet is in a non-stagnant environment, semi-empirical corrections have been suggested for the basic droplet model (26).

It has generally been assumed in implementing the coal pyrolysis analogs of droplet vaporization models that the temperature of the particle surface effectively tracks the gas temperature. This is due to the fact that net heats of coal pyrolysis are often quite modest, typically cited values being between zero and 100 cal/gm of coal (30-32), most often endothermic, but at times exothermic.

To this point, the role of convection, due to escape of light gases from the particle, has not been discussed. Certainly if this flux is sufficiently high, escape of tars from the particle surface might be enhanced by such a flow. The issue of whether the surface flux of light volatiles is sufficiently high so as to contribute to the transport of tar has been examined (25). It has been shown that the ratio of the pure diffusion flux of tar (in the absence of light gas evolution) to the flux of tar in the case of convective enhancement is:

$$\text{pure diffusion/convective enhancement} = \phi/(1-\exp(-\phi)) \qquad (2)$$

where $\phi = NR/D_V C_V$, N = true molar surface flux of all species (gas + tar), R = particle radius, D_V = diffusion coefficient of tar in the surrounding gas, and C_V = molar density of the gas phase. This of course assumes that the flux is uniform over the entire surface of a spherical particle. It was calculated that for a typical 75 μm particle, the convective enhancement is at most a few percent, but for 1 mm particles it can be quite significant.

This discussion leads into another possible mechanism of tar transport. It has been observed on occasion that volatile matter does not uniformly leave the surface of pyrolyzing coal particles. Rather, "jets" of volatiles are observed, indicating the existence of highly non-uniform surface fluxes. It has been presumed that in such a situation, the velocity of a jet of volatiles leaving the surface of a particle may be sufficiently high so that physical entrainment of tar may occur (in a high shear region, or upon bursting of a bubble at the surface). This leaves open the possibility that tar need not evaporate in order to escape the particle.

Evidence that evaporation must be a significant factor in determining the escape of tar in pulverized fuel size particles is shown in Figs. 4 and 5. Figure 4 shows the molecular weight distribution of an atmospheric pressure pyrolysis tar in comparison to the molecular weight distribution of extractable material left behind in the particle. These experiments involved pyrolyzing finely ground particles in an electrically heated wire mesh which allowed rapid escape of all vapor phase species. Clearly, there was a selective evaporation of lighter material. Physical entrainment mechanisms would predict similar molecular weights in tar and extractable residue. In addition, Fig. 4 also shows a significant difference between atmospheric pressure tar and vacuum tar produced under similar conditions. These data similarly suggest that vapor phase transport processes must be important, since it is difficult to imagine why condensed phase transport processes should be affected by variations in external pressure.

Figure 5 shows a comparison of the molecular weight distributions of atmospheric pressure pyrolysis tar from Illinois No. 6 coal, and a sample of tar which was re-evaporated from this original tar under identical pyrolysis conditions. Both

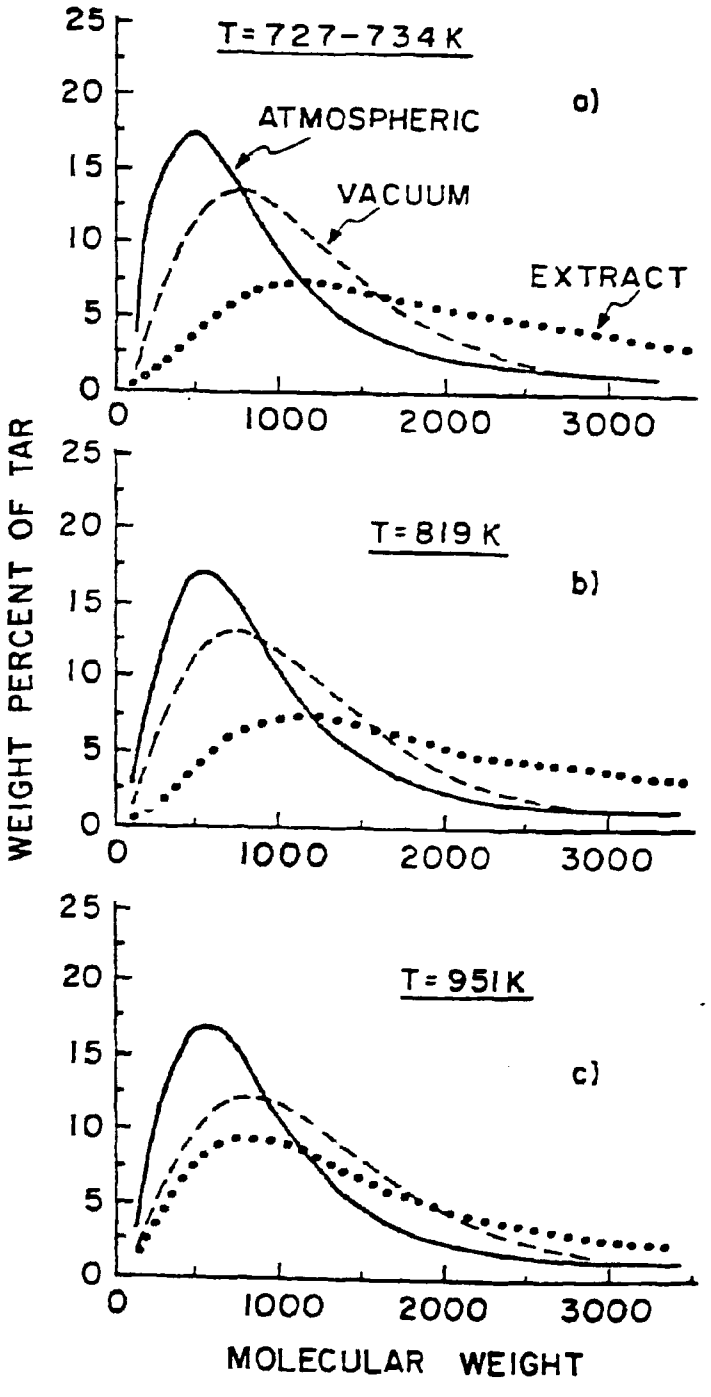

Figure 4: Molecular Weight Distributions of Bruceton Bituminous Coal Tars and Extracts. Solid curves - coal tar obtained at nominally atmospheric pressure (164 kPa); Dashed Curves - Coal tar obtained at vacuum (40 Pa) Dotted Curves -atmospheric pressure coal char THF extracts. Note that the curves are partially integrated distribution curves; the ordinate represents the weight percent of tar at any molecular weight ± 100 mass units. For example, at 819K, there is approximately 17% of the atmospheric tar within 100 units of 600 (i.e. from 500 to 700 molecular weight).[7]

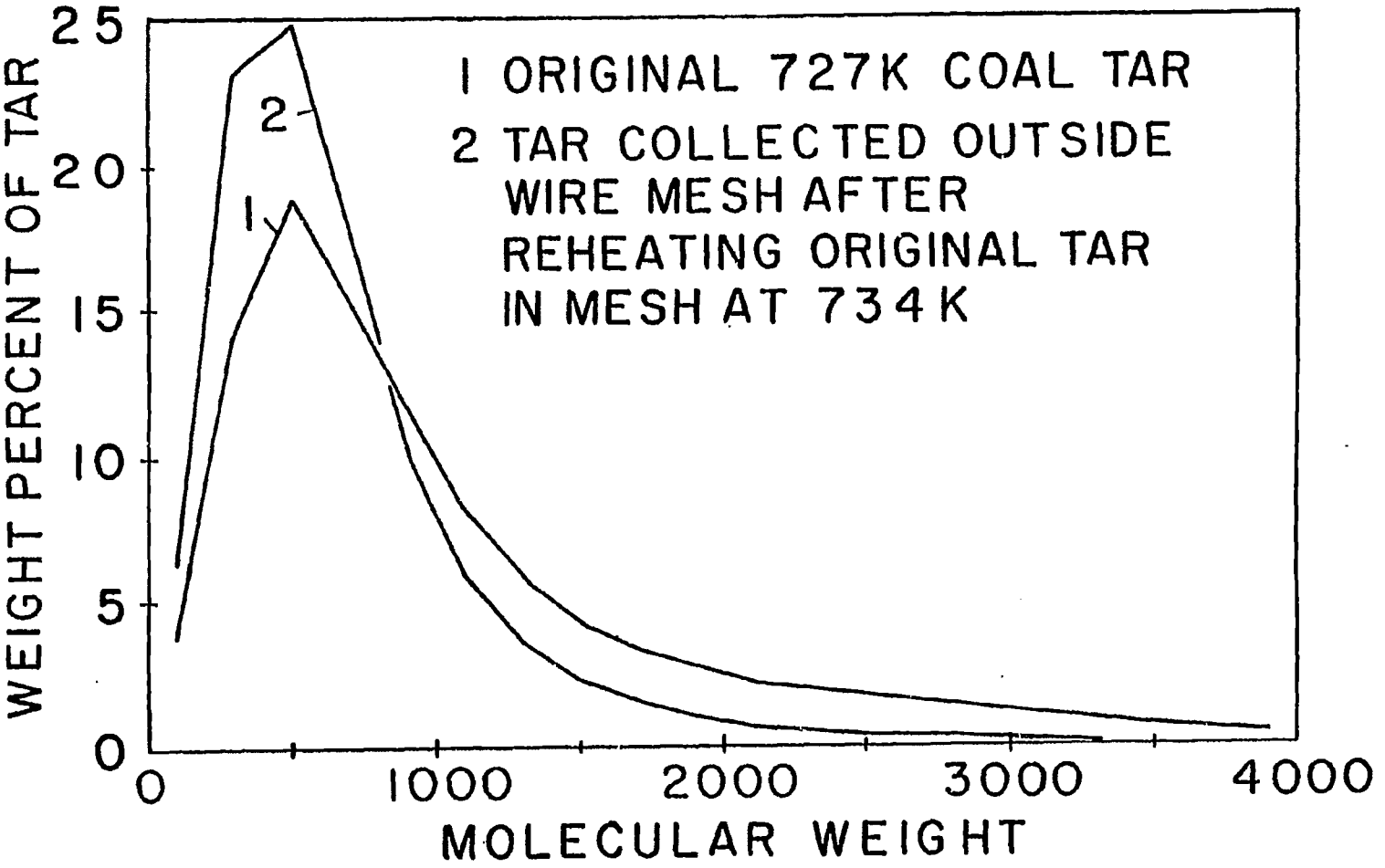

Figure 5: A comparison of the molecular weight distribution of fresh Illinois No. 6 coal tar (from pyrolysis at atmospheric pressure in helium, at heating rates of 1000 K/s) and the vaporized products of the same (pure) tar, reheated under similar conditions. Distributions are partially integrated, as discussed in Fig. 4 caption.[1]

experiments involved placing the samples (coal in one case, dry tar in the other) on the electrically heated wire mesh described above. The molecular weight distributions of the original tar and re-evaporated tar are very similar, implying that similar processes are involved in the escape of the tar in both cases. There is of course no large convective flux due to simultaneous gas evolution in the re-evaporation case, hence the conclusion that evaporation must control escape of the tar in both. The fact that the original coal tar does include more higher molecular weight material than the re-evaporated tar probably reflects the fact that there was relatively less such material in the sample of previously evaporated tar than originally present in the coal.

It is however, also possible that the presence of greater amounts of high molecular weight material in the original coal pyrolysis tar could be due to some contribution of physical entrainment. Evidence in favor of this hypothesis has been presented in the form of elemental composition data on various molecular weight fractions of pyrolysis tars (33). These are summarized in Table II, for the same Bruceton bituminous coal that was the subject in Fig. 4. It is apparent that the highest molecular weight fraction shown has such a low H/C ratio that it is rather unlikely to have escaped the particles by a vaporization process. Hence it must be inferred that this material escaped by entrainment.

Reference to Fig. 4 establishes that there is almost a third of the tar present at such high molecular weights, and thus the significance of the entrainment mechanism may be considerable.

Thus far, the discussion of molecular weight distributions of flash pyrolysis tars has focused on data obtained by gel permeation chromatography (GPC). There is some dispute as to the interpretation of these results in view of: 1) the well known problem of association of large molecules in solution and 2) discrepancy between these results and those obtained by Field Ionization Mass Spectrometry (FIMS). There is, however, no question that FIMS also reveals that the tars produced in vacuum are heavier than those produced at higher pressures (34,35). It has also been shown that the molecular weight distribution of the tars is strongly influenced by heating rate (34,36) the higher the heating rate, the broader the range and the higher the molecular weight of tars released. Thus any comparison of FIMS and GPC molecular weight distributions should be performed using the same sample of coal tar produced at comparable heating rates. FIMS suffers the possible difficulty that not all tar is vaporized during the analysis of a sample; anywhere from a few percent to over 50% might be unanalyzed typically (37). Thus it is not surprising that FIMS would tend to give lower molecular weight than GPC for comparable tars. Whether the GPC measurements are wrong due to association, or FIMS are wrong due to inability to vaporize some larger fragments as efficiently, is still open to debate. To put the problem in perspective, data on lignite flash pyrolysis tars show roughly the same most probable molecular weight of 400 daltons by both FIMS (34) and GPC (38). By FIMS analysis 99% (wt) of the tar is less than 800 in molecular weight, while by GPC, only about 50% (wt) of the tar is below this molecular weigh. For different samples of Pittsburgh Seam bituminous coal, a FIMS analysis (35) of vacuum pyrolysis tars revealed a number average molecular weight of 403, whereas GPC (39) yielded 426.

In short, both techniques confirm the key trends of tar molecular weight as a function of pressure and temperature, but there is still some question as to exactly how large the biggest fragments are that can escape the particles during rapid pyrolysis. This is an important question, since it provides a clue at to what kinds of vapor pressures might be expected for such tars.

TABLE II

Hydrogen-carbon atomic ratios of molecular weight fractions of Bruceton coal vacuum tar and vacuum chars

Molecular weight[a]	H/C atomic ratio
1642	0.83
704	1.10
391	1.09
256	0.98
220	1.03
185	1.05
Raw coal	0.80
813 K char	0.71
1043-1065 K char[b]	0.49

[a] Average molecular weight of a 2 ml elution volume fraction from preparative chromatogrphic column.

[b] Atmospheric pressure char.

Tar from different ranks of coals show differences in molecular weight distributions, as illustrated in Fig. 6 and shown in several studies (7,34,36,38-40). Generally very low rank and very high rank coals give lower molecular weight tars than do the medium and high volatile bituminous coals (38).

Evaporation control models of pyrolysis could be more extensively tested, were vapor pressure data available for coal tars. Unfortunately, such data do not exist for these substances or any heavy hydrocarbons with significant heteroatom contents. Part of the difficulty in obtaining such data lies in the fact that these materials thermally degrade at the temperature of interest. Nevertheless, attempts have been made to evaluate evaporation controlled processes by using a vapor pressure correlation of form (24,33,39):

$$p^0(atm) = 5756 * \exp(-255 * MW^{0.586}/T) \qquad (3)$$

where MW is the molecular weight and T is in K. This correlation was derived from data on miscellaneous high molecular weight hydrocarbons (containing no heteroatoms) and should certainly not be assumed to be better than an indication of the order of magnitude of the pure component vapor pressure. This is clearly an area awaiting further developments.

The above correlation would imply that a tar species of molecular weight 2000 might have a pure component vapor pressure of less than a mircotorr at 723 K (450°C). In as much as small amounts of material of this molecular weight appear to be present in low temperature pyrolysis tar samples (see Fig. 4), it is possible that either the vapor pressure prediction is incorrect, or again, that a small amount of tar is physically carried from the surface.

There is likewise a difficulty in obtaining data on vapor phase diffusivities of the tar species. However, it is felt that standard group additivity methods (e.g. Fuller-Schettler-Giddings, 41) should be applicable (42), at least at the level of accuracy required.

4.0 Internal Mass Transfer Limitations

There exist widely varying viewpoints concerning the nature of transport of volatiles within coal particles. The discussion of internal transport must always be focused first by considering whether the coal in question is softening or non-softening. In the case of softening coals, it appears to make sense to treat the particle as a liquid droplet during part of the pyrolysis process. In the case of non-softening coals, the transport of volatiles within the particle will most likely occur along pores. Unfortunately, it is difficult to predict whether or to what degree a particular coal will soften in any situation.

4.1 Softening Coals

Coal is commonly thought of as a brittle elastic solid under ordinary ambient conditions. But even under these conditions, finely ground coal particles (50 μm or less) can behave more like thermoplastic resins, in that they display permanent deformation under high shear (43). Under elevated temperature conditions (i.e. 650 K and higher), many types of coals show much more easily discernable fluidity or plasticity. Generally this high temperature plasticity is seen only in coals of greater than 13 to 15% volatile matter, and is usually not observed in coals whose ASTM volatile matter yields exceed 40% (44). Various other factors, however, can play a role in determining whether a coal softens during pyrolysis (e.g. see reviews in 44-47). It has been reported many times that the rate at which a coal is heated determined its fluidity. Generally, the higher the rate of heating, the more fluid coal becomes, and the wider the temperature range over which fluidity is

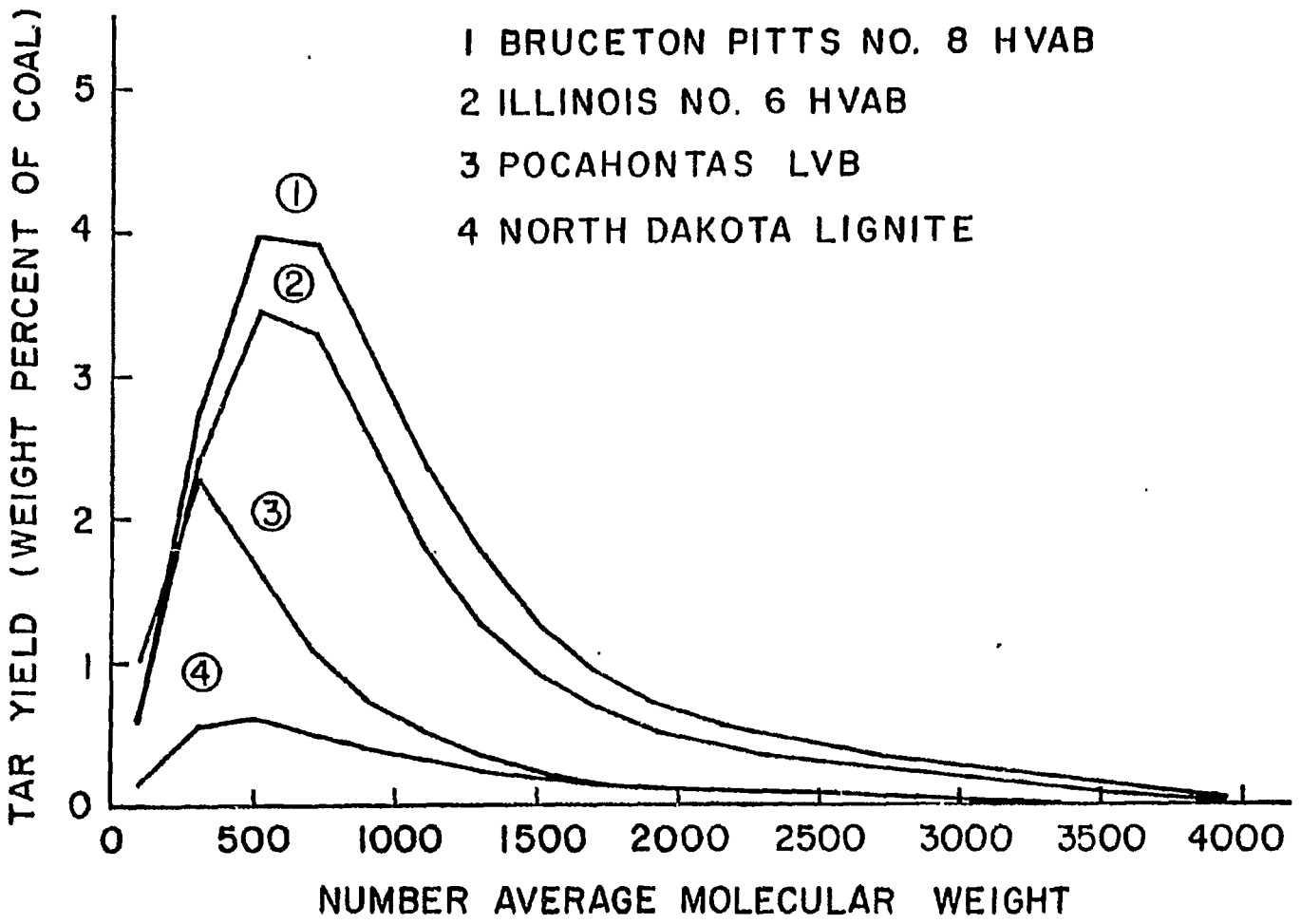

Figure 6: Molecular weight distributions of tars from different ranks of coal. All results obtained at nominally atmospheric pressures of helium (164 kPa), at temperatures above 1080K. Distributions are partially integrated as discussed in Fig. 4 caption.[7]

observed. In fact, very rapid heating of lignites and brown coal macerals resulted in apparent plasticity of these normally non-softening materials (48,49). The gaseous environment also has an enormous influence on the fluidity of the coal; increased pressure and the presence of hydrogen during pyrolysis both tend to increase the tendency of coals to soften and become fluid (including making softening coals out of otherwise non-softening coals). On the other hand, pre-oxidation enormously decreases softening tendency.

It is fair to say that the processes involved in development of fluidity in coal remain poorly understood. The problem is partly due to the heterogeneity of coal. Different maceral compounds can exhibit markedly different softening behaviors. For example, a coal which is mainly composed of infusible vitrinite may be softened by the action of exinite components, which are thought to act as "plasticizers" (44). A plausible explanation of the plastic properties of coal, based on depolymerization mechanisms, has been advanced based on work with model systems (45,50). The extent of crosslinking of the parent material has been shown to be a key factor in determining softening and tar forming tendency.

In its high temperature fluid state, coal is decidedly non-Newtonian in behavior (51). Measurements of the fluidity are normally performed in high temperature rotating-arm viscometers (Geiseler plastometers), and results are expressed only in units pertaining to that particular device. The ordinary concept of viscosity has little meaning in such systems, since not only is the fluid non-Newtonian, but it is full of bubbles and suspended solids during measurement (recall that the coal is pyrolyzing at the time). Where attempts have been made to calibrate such a devise against known standards, minimum apparent viscosities of highly fluid coals are in the range of 10^4-10^5 poise under slow heating conditions (45).

A recent study on plasticity of rapidly heated coals has shown that as much as 80 wt% of a Pittsburgh Seam bituminous coal becomes fluid (either extractable or volatile) during pyrolysis (52). The peak in yield of pyridine extractables coincides well with the rapid decrease in apparent viscosity of the softened coal. At heating rates of order a few hundred to one thousand degrees per second, apparent viscosities ranges from a few thousands to one million poise (53), which values are at the low end of range observed for very fluid coals at slow heating conditions. The effect of either increasing or decreasing pressure from atmospheric was to generally decrease the plastic period.

Despite the very high values of apparent viscosity cited above, many coals are sufficiently fluid during pyrolysis so as to lose virtually all solid structural identity. Generally, these are exactly the same coals that exhibit highest tar yields, and thus greatest absolute sensitivity to mass transfer effects. Of course all these materials begin and end the pyrolysis processes as solids, and there might be a question regarding whether the period of softened behavior coincides with the period of significant tar evolution. It has, however, been observed under rapid heating conditions (1000 K/s) that a bituminous coal displays evidence of softening at a temperature of about 650 K, prior to the evolution of the majority of the tar (5). More recent work has shown softening at a constant temperature of 580 K, independent of heating rate near 1000 K/s (53). Hence it appears to make sense to view the transport of pyrolysis products through softening coals in terms of liquid phase processes rather than pore diffusional processes.

Within a softened coal particle, two mechanisms of transport of tar species from bulk to surface must be considered-ordinary diffusion and convection. Again because of the general paucity of physical property information, it is difficult to be quantitative about either mechanism. With regard to convection, the initial assumption of no gas-particle relative motion necessarily implies that there will be no drag-induced circulation within the particles. Even if there were

significant gas-particle relative motion, it is not likely that the internal circulation would be very vigorous given the highly viscous nature and small diameter of the particles (for a discussion of how induced circulation affects vaporization of multi-component droplets, see for example Ref. 54).

Another possible mechanism of convective mixing within a softened coal particle involves the passage of bubbles through the particle. Whether the bubbles can provide a large amount of physical mixing is unclear. The very viscous nature of the surrounding medium suggests that motion of the fluid may not be very vigorous, but of course it is difficult to predict what the dynamics of such processes as bubble growth, merger and surface breakage might be, particularly since the fluid properties are unknown to even an order to magnitude. Again, the above cited minimum apparent viscosities are for a slowly heated coal, not for the rapidly heated material of interest here. Surface tension is likewise unknown for such materials, but has been estimated to be of order 10 to 100 dyne/cm (55,56).

In addition to providing physical agitation in the liquid phase, bubbles can also transport volatile species from the bulk to the surface as vapor species. This latter mechanism would reduce the distance that a tar species would have to diffuse through the liquid before evaporating. A semiquantitative analysis of homogeneous bubble nucleation processes in coal melts has been performed, and showed that the tendency to nucleate bubbles should decrease with decrease in particle size (55). It seems unlikely that homogeneous nucleation phenomena should control bubble formation, however, as there are a myriad of solid surfaces with irregular surfaces in coal particles (ash particles, infusible macerals, etc.). Nevertheless, the competition between diffusion of vaporizable species to bubbles vs. the particle surface should determine the growth rate of bubbles and thereby, their importance in transport of volatiles.

It has been claimed that transport of tars to bubbles (with subsequent escape of the bubbles) must be a primary mechanism of transport of tars out of softened coal particles (4). This conclusion was based on a liquid phase diffusivity estimated to be of order 10^{-14} sq cm/sec, to be discussed below. The alternative to this combined diffusion/convection escape route is the pure diffusion route, whereby the tars escape by diffusion to the surface of the particle, regardless of whether bubbles exist or not. The importance of one mechanism relative to the other would depend heavily upon bubble dynamics within the particle. In the limit of very few small bubbles, liquid diffusion to the particle surface must control; if on the other hand many large bubbles purge the particle frequently, the characteristic length for liquid phase diffusion of a tar species is much smaller than the particle diameter.

In considering the role of liquid phase diffusion processes, there is a major problem of lack of liquid phase diffusion coefficient data. Many measurements have been made on the rates of methane diffusion in solid coals at ambient conditions (57-60). Diffusivities which range anywhere from 10^{-5} to 10^{-15} sq cm/sec may be calculated from these data. Measurements of CO_2 and argon diffusivities range from 10^{-7} to 10^{-9} sq cm/sec (61). There appears to be general agreement that the diffusion of such gases in coals tend to be an activated process, with an activation energy of order 1 to 10 kcal/mole. Of course these data are for systems quite different than that of present concern. The only estimates of diffusion coefficients in common use for systems which resemble softened coal are those for diffusion of hydrogen in coal liquids, typically assumed to be of order 10^{-5} sq cm/sec (e.g. Ref. 62). Again, it is questionable whether such values have relevance for diffusion of tars in softened particles.

Given the shortage of relevant data, it has been suggested that the Stokes-Einstein equation might be suitable for estimation of tar diffusivities, and is the origin

of the 10^{-14} sq cm/sec estimate cited above (4). Unfortunately this estimation technique relies upon having a good estimate of softened coal viscosity, which of course is not readily available. Also, the Stokes-Einstein equation can rigorously only apply to situations which there is diffusion of a large solute relative to small solvent molecules (which may be treated as a continuum). Since there exists no such disparity of molecular sizes in the present situation, the equation is of questionable applicability. Measurements of the diffusion of naphthalene in high viscosity oils have clearly shown the Stokes-Einstein equation to be invalid (63). The diffusion coefficient was found to vary inversely with viscosity to the 2/3 power in the above study, as opposed to inverse first power as predicted by Stokes-Einstein. It was found that naphthalene (MW = 128) has a diffusivity of about 3 x 10^{-5} sq cm/sec in 50 poise oil at 298 K.

It is without question very dangerous to extrapolate the above data to the conditions of present interest; nevertheless it is useful to do so only to get an estimate of a reasonable order of magnitude of diffusivity. Assuming that the viscosity of the coal may be taken as 10^4 poise it can be estimated that the diffusivity of naphthalene would be of order 10^{-9} sq cm/sec at 1000 K. This is in agreement with an estimate which may be made from an empirical correlation for self-diffusion coefficients of hydrocarbon liquids (64).

$$D_L = 6.3 \times 10^{-8} (T/T_b)^{0.7805} T/(\mu)^{2/3} \qquad (4)$$

where D_L is in sq cm/sec, T and T_b (the boiling point) are in K, and viscosity μ is in cp. It is assumed that the term involving boiling point is of order unity at 1000 K. The examination of a correlation for self-diffusion is appropriate inasmuch as the tar is assumed to consist of oligomers of not very widely differing molecular weight.

Finally, it should be mentioned that Hershkowitz has estimated a diffusivity for tar to be of order 10^{-6} sq cm/sec (65). This estimate was based on measurements of diffusivities of asphaltenes (66). On these grounds, it appears that the appropriate range of diffusivities for tars should be of order 10^{-6} to 10^{-9} sq cm/sec.

On the basis of such diffusivities, it may be surmised that even with particles as finely ground as those in Figs. 1-4 (of order 10^{-2}cm), the time scale for tar to diffuse out of the particles unassisted by bubbles would necessarily be of order (R^2/D_L =) 10 to 10^5 sec. This is longer than the actual time required for the pyrolysis process to achieve apparent completion (order 1 to 10 sec under typical high heating rate, high temperature conditions). The latter time scale is undoubtedly dictated by the rates of chemical reactions rather than diffusion. However, as will be shown later, a diffusion coefficient of 10^{-6} sq cm/sec may still be high enough to allow escape of a realistic amount of tar, even if a significant amount is trapped in the particle.

It is also instructive to compare the magnitude of the internal and external diffusional processes. Again neglecting the role of bubbles, it has been shown (24,25) that the relative time scales for internal and external diffusion must be:

$$t_i/T_e = D_V C_V y/D_L C_L x \qquad (5)$$

where D_V and D_L are the vapor and liquid phase diffusivities of the tar species, respectively; C_V and C_L are the vapor and liquid phase molar densities; and y and x are the vapor and liquid phase mole fractions of tar. Assuming Raoult's Law, if P^o is the vapor pressure of any pure tar species, $y/x=P^o/P_{tot}$. P_{tot} is the pressure external to the coal particle. The ratio (C_V/C_L) is of order 10^{-2} to 10^{-3}. Based on the above estimates of diffusivities, (D_V/D_L) is of order 10^5 to 10^9. This

means that unless (P^o/P_{tot}) is of order 10^{-3} or less, internal diffusion is likely to control the rate of tar escape.

Employing the previously presented vapor pressure equation, for "typical" tar molecular weights of 300 to 2000, at 700 K, the quantity (P^o/P_{tot}) would range from 10^{-1} to 10^{-10}; at 1000 K, the range would be from unity to 10^{-6}. On this basis, it is apparent that either gas phase diffusion or liquid phase diffusion might control, depending upon both the temperature and the molecular weight of the species in question (lower molecular weights and higher temperatures tend to favor internal mass transfer control). Enhancement of liquid phase transfer processes by bubbles would increase the likelihood of external film diffusion control.

The observed pressure dependence of tar yields cannot be explained if pure liquid phase diffusion controls escape of the tars. It was just such a pressure dependence that initially suggested use of an evaporation-gas film diffusion control model of tar escape. The pressure dependence does not unequivocally establish the case for external gas film diffusion, however. If bubbles transport the tar from the bulk of the particle to the surface, then the pressure dependence might be explained in terms of slower bubble growth and escape rates with increasing external pressure (56). As previously noted, in this case true liquid phase diffusion of tar may have to occur over only a short distance, to the nearest bubble (4).

What is difficult to rationalize by a bubble-escape-limited model is the very definite shift in molecular weight distributions of pyrolysis tars with pressure (see Fig. 4). If bubbles, by virtue of intimate contact with the coal melt, are equilibrated with respect to all tar species, then variations in external pressure should have no effect on relative concentrations of different molecular weight tars within bubbles (assuming that the mole fraction of tar in the bubbles is low; estimated from overall pyrolysis product compositions (5) to be no more than a few percent).

The weight of experimental evidence presented to this point seems to favor external gas film control of tar escape from softened coal particles. The data in Fig. 7 show that the process is not as straightforwardly analyzed as multi-component droplet evaporation, however. Figure 7 shows the variation of the molecular weight distributions of tars evaporating from Pittsburgh No. 8 bituminous coal (7), as a function of different temperature ranges of pyrolysis. Surprisingly little temperature dependence is observed, although the shift towards higher molecular weights with increasing temperature is expected. A much more dramatic shift has been predicted based on essentially a "batch distillation" model. Low temperatures should favor the evaporation of light species, and higher temperatures should favor the evaporation of progressively heavier species, as light species become exhausted. Such predicted behavior is shown in Fig. 8, based on an existing model of softened coal pyrolysis (39).

The absence of the predicted dramatic temperature dependence has been attributed to the superposition of chemical reaction phenomena on the multi-component evaporation process. In the pyrolytic reaction rate controlled evaporation case, the various low molecular weight classes are continually replenished by chemical reaction at the same time that evaporation is occurring. Evidence of this is presented in Fig. 9, which shows the simultaneous variation of tar and extractable material with pyrolysis temperature (extractable material here can be viewed as identical to tar, expect that it has not yet escaped the particle; it is recovered by extracting the particle with a suitable solvent after the pyrolysis experiment). It is apparent that under the rapid heating conditions employed, the sum of extractables and tar increased continually with increasing temperature. Earlier it had been believed (6,25) that the reactions which formed the tar precursors occurred very quick

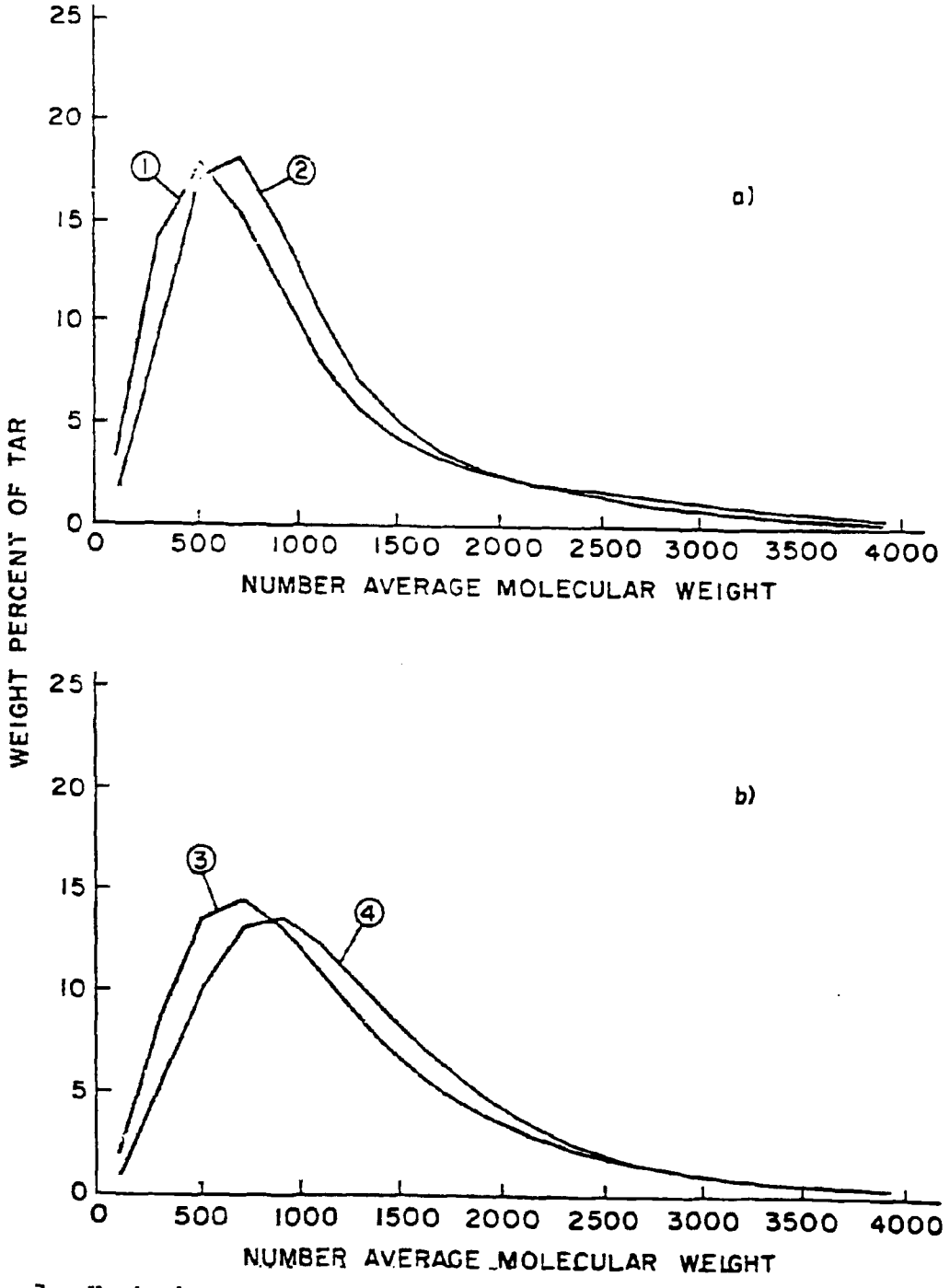

Figure 7: Variation of Molecular Weight Distributions of Bruceton Coal Tar as a Function of Temperature of Evolution. a) Atmospheric pressure tar (164 kPa); b) Vacuum tar (40 Pa). Curve 1) Tar evolved between room temperature and 727 K (roughly 10 mass percent of the coal); 2) Tar evolved between 727 and 819 K (an additional 8 mass percent of the coal); 3) Tar evolved between room temperature and 659 K (roughly 5 mass percent of the coal); 4) Tar evolved between 659 and 727 K (an additional 8 mass percent of the coal). Distributions are partially integrated, as discussed in Fig. 4 caption.[7]

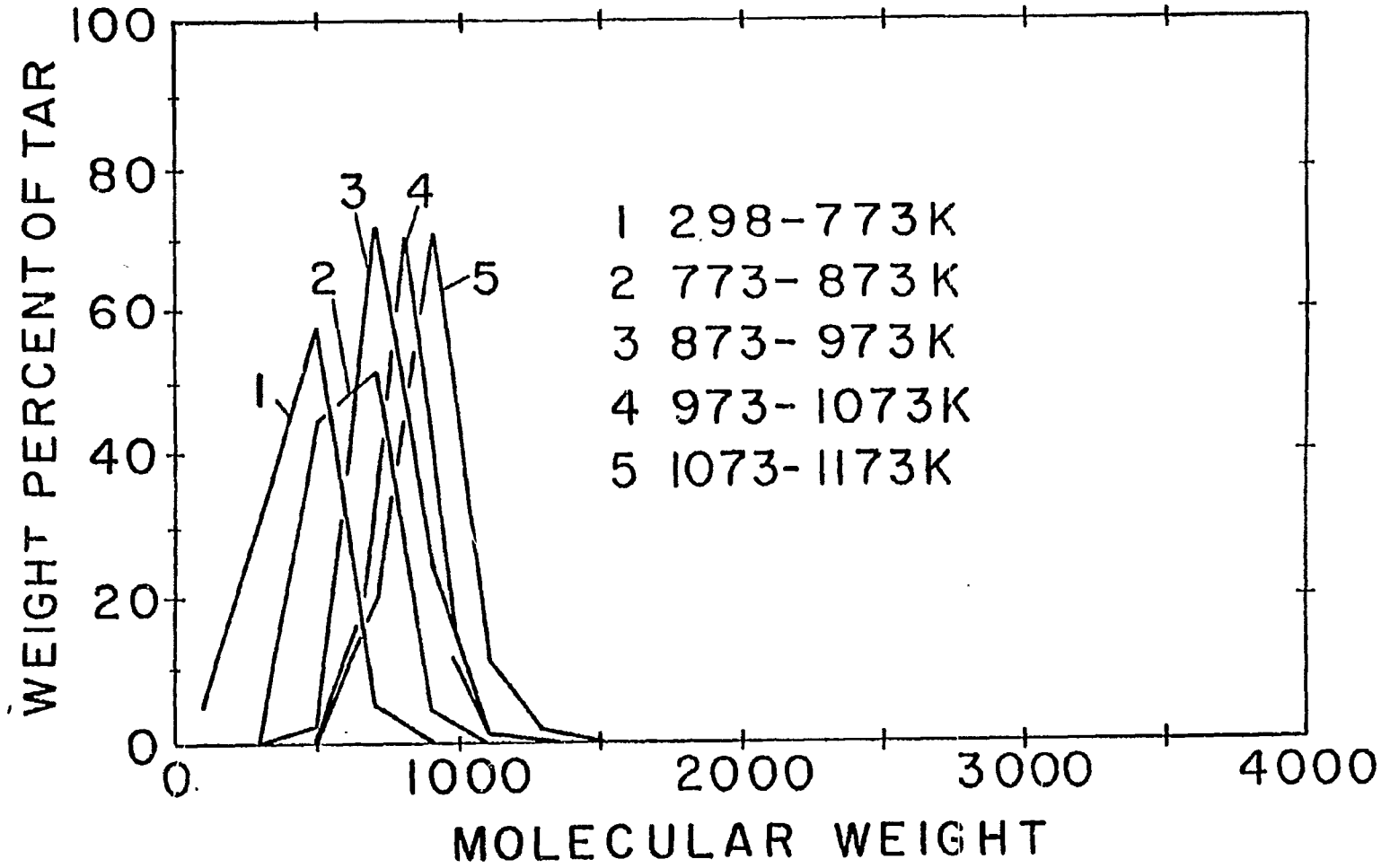

Figure 8: Predictions of a "batch distillation" type pyrolysis model. Partially integrated molecular weight distributions, showing the distributions of tars evolved between the indicated temperatures. There is a clear shift towards significantly higher molecular weight with temperature. This model considerably overpredicts temperature variations in tar distributions such as those seen in Figures 4 and 7.[39]

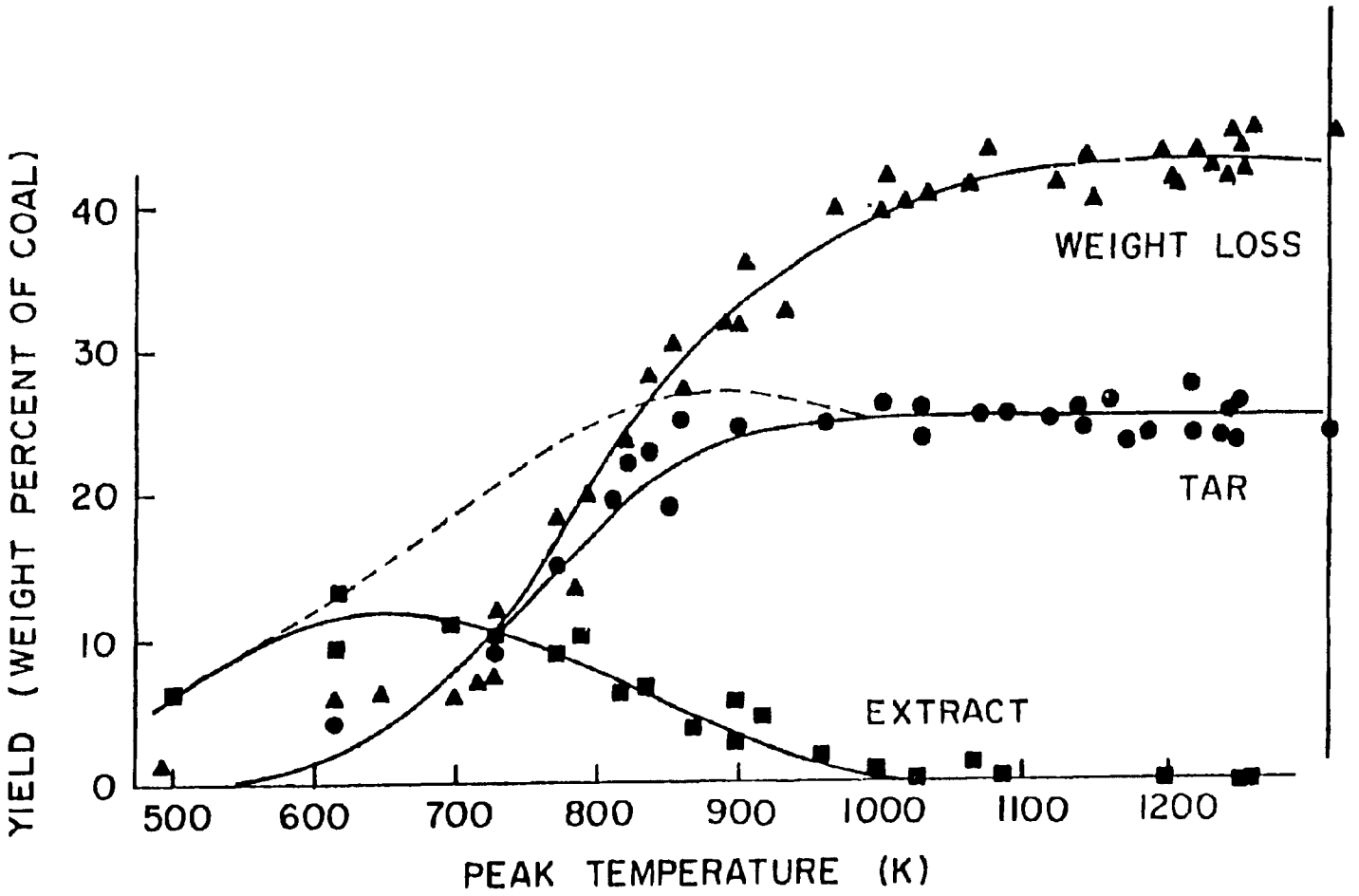

Figure 9: Weight loss, tar yield, and extract yields from pyrolysis of Bruceton coal at 1000 K/s to indicated temperature, under atmospheric pressure of helium. Dashed curve represents the sum of tar plus extract yield.[7]

prior to evaporation of any tar. In view of Fig. 9, it must be concluded that the "pool" of evaporable tar is constantly being replenished throughout the period of most active tar evaporation.

Consequently, the weight of experimental evidence favors a process of tar escape which is partly controlled by the rate at which evaporable species are formed and partly by the evaporation rate of these species once formed. This is the assumption upon which several recent models of coal pyrolysis are based. These will be discussed below.

4.1.1 Changes in Particle Morphology During Softening

There are two important aspects to this problem, one having to do with changes in the fine porous structure of softening coal particles, and the other with changes in the gross morphology of the entire particle itself. The latter issue will be explored first.

Cenosphere Formation - Under certain conditions, particles become fluid enough and gas evolution rapid enough such that the particles "balloon" into so-called cenosphere structures with diameters many times those of the original particles (see discussions in Refs. 3 and 67). This phenomenon is also only qualitatively understood, and many contradictory claims exist concerning the effects of various factors on the behavior (particle size, heating rate, etc.). From a sampling of data on a variety of coals showing such behavior, it appears that with the finely ground particles of interest here, diameters may typically be expected to increase by a factor of 1.5 (67). Not all particles will tend to swell, although a significant fraction often do (68-72). The ambient gas has a significant influence on the swelling tendency. In air, the increase in diameter of coals rapidly heated in a drop tube was typically less than a factor of 1.2, whereas in N_2 the factor was seen to be between 1.16 and 1.6 (69). In other recent similar studies, the diameters of particles were observed to increase by a factor of as much as 4, in inert gas (70). Steam slightly decreases the tendency to form cenospheres, while coal gas and hydrogen seem to have little effect, compared to inert gas (71). The influence of coal rank on swelling behavior, is of course, well established (67-69, 71, 73) but standard swelling tests appear to be poor indicators of extent of swelling under high heating rate conditions (68,69). The standard low heating rate swelling test has been noted to depend upon the particle size examined, with smaller particles swelling relatively less than larger particles (74). This is contrary to the findings of another study that found rapidly heated particles in the 400-700 μm size range swelled less than those in the 50-100 μm range (73). Another study also revealed increased swelling with decreased particle size in the range 100 μm to 1000 μm (75). A previously cited study, however, indicated little effect of particle diameter, in the range of 24-105 μm (69). This again is contradicted by data in a recent thesis, which reported that in inert gas, Pittsburgh Seam particles of 45-54 μm diameter are less prone to swelling than 20-25 μm particles (76).

Recent studies of coal plasticity have also suggested that the plastic properties are not only a function of coal type and heating rate, but of **absolute** pressure as well (77,78). Increased rate of heating has already been noted as a factor in determining higher plasticity, but there is only scattered evidence to support the viewpoint that increased rate of heating leads to higher swelling ratios (73). In fact, some data from a laminar flow reactor in which very high temperatures (2100 K) and high heating rates were examined suggest that **no** swelling occurs in devolatilization of a highly softening coal (up to a mass loss of 60% wt) (79). Examined at lower temperatures (1510 K) in the same device, the Pittsburgh Seam coal of original 60 μm diameter swelled to an average diameter of 450 μm.

In the face of such confusing and sketchy experimental evidence on swelling, it is still difficult to construct very robust models of swelling behavior. Until a reliable set of data are available for validation of any model, it is clear that progress will be hampered. Nevertheless, progress on modeling of swelling is important, and some attempts are outlined below.

Obviously, a large amount of cenosphere formation during devolatilization could have a large effect on mass transfer, both during devolatilization and subsequent gasification. But it has never been clearly established how crucial the accuracy of such models might be in any situation. Obviously, several factors are affected by cenosphere formation:

- The aerodynamic drag on the particle is altered, as the particle becomes larger (and of course, less dense).
- The heat transfer surface of the particle is increased, and its interior thermal conductivity changes.
- The external surface for mass transfer is increased, and the internal surface area may also change. Bulk gas phase transport becomes more important in the particle interior.

Some features will be much more sensitive to swelling than others. Most obviously affected are quantities such as the particle Reynolds number, which is proportional to diameter. But unless slip velocities between particle and gas are large, the Nusselt number for heat transfer or the Sherwood number for mass transfer are not much affected by small changes in size when particles are of order 100 μm in size. This is because for particles of 100 μm in size, the Reynolds numbers in pulverized coal flames are not expected to exceed 100, and will generally not exceed even unity. For example, the kinematic viscosity (μ/ρ) of air at 1800 K is roughly 3 cm^2/s, and even with a high slip velocity of 10 m/s between particle and gas, a 100 μm particle would have a Reynolds number of Re = $\rho VD/\mu$ = 3.3.

Commonly applied correlations for the Nusselt number for spherical coal particles are exemplified by (80)

$$Nu = 2 + 0.654\ Re^{0.5}\ Pr^{1/3} \qquad (6)$$

This means that, given a Prandtl number for air of 0.7, the Nusselt number would go up by a factor of only 14% with a doubling in particle size, implying an increase of a factor of just over 2 for the actual heat (or mass) transfer rate due to conduction/convection, despite the factor of four increase in surface of the particle.

Radiative transfer to/from the particle will scale with the surface area, and thus go up by a factor of four with a doubling in size. It is apparent that if the maximum swelling is as modest as some studies have suggested it is in air (~10%) and if slip is small, then convective rates of transport will not be affected much by inaccuracies in a swelling model. The radiative transport rate will be more significantly affected, but whether this is important or not depends upon the relative importance of radiative and convective heat transfer in a particular situation (generally radiation is more important, the larger the particle).

For more complete discussion of the issues involved in calculating transport rates to and from particles, the reader is referred to the extensive reviews in Refs. 81-83.

Thus far, no mention has been made of the change in porous structure that accompanies the softening and swelling of coals. Discussion of this issue will be reserved until the presentation of material concerning non-softening coals. Instead, attention will be turned first to the modeling of softening coal pyrolysis and the macroscopic swelling phenomena.

4.1.2 Modeling of Softening Coal Pyrolysis

The majority of presently available pyrolysis models do not explicitly account for the observed effects of external gas pressure or particle diameter on yields. Since many applications of these models involve conditions not very different from those from which their pseudo-kinetic constants were derived, the problem of failure to account for mass transfer limitations is sometimes not important. The extrapolation of such models to significantly different particle sizes, pressure conditions, or heating rates can however be dangerous.

Of the models in the literature which do account for mass transfer effects, several involve only predictions of weight loss (17,56,84-88). Of these, some have modeled the transport processes by use of an empirical external mass transfer coefficient (17), some by invoking pore transport (84,88), some by postulating transport controlled by bubbles within the particle (56,86,87), and one employed both a crude model of pore diffusion and an external mass transfer coefficient (85).

Initially, we consider only those models that pertain to softening coals.

Anthony et al. (17)

Anthony et al. (17) considered pyrolysis of bituminous coal as involving formation of two kinds of volatile precursors within the coal particles-"reactive" (qualitatively associated with the tar species) and "non-reactive" (fixed gases). The general outline of the model is given below:

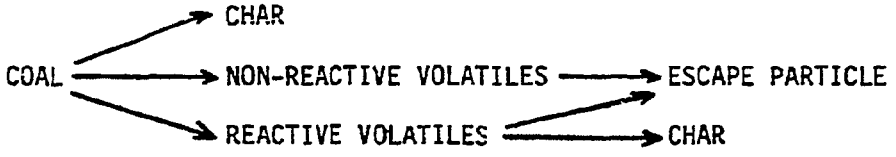

The change with time in concentration (C) of the reactive volatiles within the particles is represented as:

$$dC/dt = Q_r - K_m C - k_r C \qquad (7)$$

where Q_r is the formation rate of reactive volatiles (mass per unit mass of coal); K_m is a rate of "deposition" or "repolymerization" reactions within the particle. Both the mass transfer process and the reactive volatiles repolymerization processes are thus modeled as first order in reactive volatiles. It is assumed that a quasi-steady state exists for the concentration of reactive volatiles ($dC/dt = 0$). On this basis, $C = Q_r/(K_m+k_r)$, and thus the rate of mass loss of reactive volatiles (m_r) is given by:

$$m_r = K_m C = Q_r/(1+k_r/K_m) \qquad (8)$$

Integration of this expression over time yields the total amount of reactive volatile which escapes the particle during an experiment. Assuming the ratio k_r/K_m to be independent of time, and letting Q^* represent the integral of Q_r over time, then the actual fractional mass of reactive volatiles (per unit mass of coal basis) to escape the particle is:

$$V_r = Q^*/(1+k_r/K_m) \qquad (9)$$

It is suggested that K_m should be proportional to an ordinary bulk diffusion coefficient, which varies inversely with pressure. Hence a pressure dependence is postulated for V_r. The total yield of volatiles (on a per unit mass of coal basis) is given by the sum of V_r and V_{nr}, where the latter term represents the fractional yield of non-reactive volatiles, on a per unit mass of coal basis. The quantity V_{nr} is not a function of pressure.

The above model was used to fit a curve of weight loss vs. pressure which quite closely resembles that in the top most section of Fig. 1. In order to obtain such a fit, it was necessary to take $Q^* = 0.17$, $V_{nr} = 0.37$, and $k_r/K_m = 0.56$. There of course is no a-priori means of predicting these values. Nevertheless, the success of this simple model in predicting the trend of the mass transfer effects has suggested a search for a more fundamental transport model which involves the inverse pressure dependence of ordinary diffusion.

Mills et al. (86,87)

These models pertain only to softening coals, and consider only transport processes internal to the particle. It was initially postulated by Mills et al. (86) that the pyrolysis process involves reactions to form primary, secondary, and tertiary gas species (PG, SG, TG); intermediate solid coal and softened coal (IC and M- the latter symbol representing "metaplast"); and both semi- and final coke (SC and C). The general structure of the proposed model was:

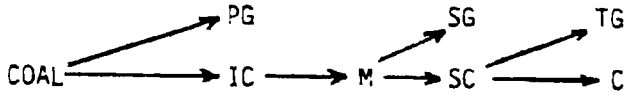

The tars were postulated to be part of the PG and SG fractions. Ordinary first order rate expressions were used to described the reactions of the pseudo-species named above. No attempt was made to differentiate between different products of pyrolysis, so the pseudo-species merely represented parameters in a weight loss model. In this early implementation of their model, Mills, et al. focussed mainly upon particle swelling phenomena. The model involved prediction of extents of swelling via an empirical "foaming law", which related the specific volume of the bubble containing metaplast (v_m) to the gas mass flux within the particle (G):

$$v_m = (1 + fG)/\rho \qquad (10)$$

where f is a foaming constant and ρ is the initial density of the coal (a reference density). As the gas flux increases, it is clear that a greater extent of swelling is predicted. The swelling process is pictured as limited only by the rate of gas evolution, and by the extent of total mass loss from the coal. No explicit account was taken of gas bubble escape followed by surface tension driven collapse. As a result of the empirical approach taken here, there is no a-priori way of predicting swelling behavior in a coal for which measurements are unavailable.

In the more recent version of the model proposed by this group, it is assumed that the heavy vapor species (tars) are always in equilibrium with the condensed phase within the particle, and that these species exist within bubbles (87). Few details of the equations governing this vapor-condensed phase partitioning are provided. The reaction scheme has been slightly modified in this case as well, and reflects the competition between escape of the tars and their repolymerization into the coke:

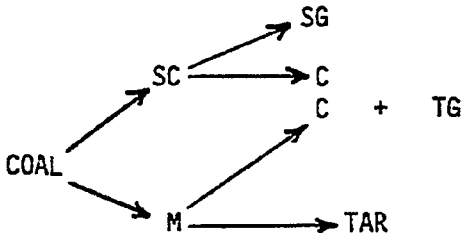

The nomenclature shown here is consistent with the first version of the model. Also, several other model structures have been explored; that shown here is among the more "realistic".

The transport of pyrolysis products vis bubbles is governed by the rate of bubble motion relative to the condensed phase (V_b), where

$$V_b = K_1 (1- \mu') (dP/dr) \qquad (11)$$

The bubble velocity is thus assumed proportional to the pressure gradient within the particle (dP/dr). This gradient is set up by the evolution of gaseous species within the particle. The quantity μ' is a normalized viscosity ($\mu' = 1$ is a solid), and K_1 is a proportionality constant. Vapor is also permitted to flow by an unspecified separate mechanism outside of the bubbles; the velocity relative to the condensed phase is:

$$V_g = V_b - K_2(dP/dr)/(1-K_3 \mu') \qquad (12)$$

where K_2 and K_3 are again empirical constants. Presumably this equation represents an empirical treatment of pore transport prior to softening. In this implementation of the model, swelling is nominally allowed for by considering growth of bubbles; however it was claimed that unreasonable results were obtained and the swelling equations were dropped (the implications for the bubble transport picture have not been discussed).

While this second model apparently gives realistic trends of volatile mass yields with pressure, no validation against experimental data has been attempted. No sensitivity analyses have been reported on the large number of adjustable parameters.

Lewellen (56)

This model involves a description of transport in softening coals. The focus is almost entirely upon internal transport of volatiles via bubbles (although a small allowance is made for direct escape of volatiles from the surface). It is assumed that coal particles are essentially isothermal, viscous liquid droplets. All volatiles are assumed to be the same in molecular weight and chemical nature. The general structure of the transport and reaction model is as shown below:

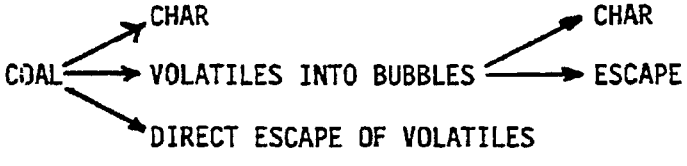

Once formed, the volatiles within a particle can either escape from the surface of the particle directly or enter a bubble; the ratio of volatiles escaping the particle to those entering bubbles was assumed proportional to the ratio of particle surface area to internal bubble surface area. Volatiles leave bubbles in

either of two ways, by repolymerization on the surface of the bubble (to form a coke precursor) or they escape to the surrounding atmosphere when the bubble breaks the particle surface.

The strong feature of this model is the attempt to treat the fluid mechanics of particle swelling and growth in a realistic yet mathematically tractable manner. Bubbles are assumed to nucleate throughout the particle in a stochastic manner. Growth of each bubble is governed by the magnitude of the pressure gradient between the bubble and external environment, and is evaluated based on the shortest distance between the surface of the bubble and the surface of the particle. Analogy is drawn with the process of blowing up a balloon with a thin spot; growth will always be most rapid at that location. Bubble growth rates are thus given by:

$$\frac{dr_b}{dt} = \frac{r_b(P_b - P_o) - 2\sigma\left[1 + \frac{r_b}{w_b}\right]}{4\mu\left[1 - (r_b/w_b)^3\right]} \qquad (13)$$

where r_b = bubble radius; P_b,P_o = bubble and ambient pressures; σ, μ = coal melt surface tension and viscosity; and w_b = shortest distance from particle surface to bubble. As noted earlier, mass is added to each bubble at a rate proportional to its surface area, and the total mass of the bubble determines P_b.

Bubbles are assumed to grow independently of one another until two intersect (defined by the instant that two develop a point of tangency on the expanding grid system used to describe the particle). At that moment, the two bubble masses are merged and a new single bubble of equal mass is created at the center of mass of the former pair. The new bubble is stationary at the moment of formation. The escape of bubbles from the particle occurs when they come within a certain arbitrary distance of the particle surface, (a critical film thickness is defined).

While admittedly not a highly refined model, it shows a great deal of insight into the mechanics of bubble transport and should be quite valuable as a guide to future developments along these lines. In its present form, the model does successfully predict trends such as repeated particle swelling and collapse. Realistic diameter increases, in the range of 1 to 3, were predicted assuming viscosities of order 10^6 poise and a surface tension of 50 dyne/cm. The general trends of volatile yield with pressure are to some extent correctly predicted, although problems were encountered in certain cases. It is not surprising that better success was not achieved, given the crude assumptions concerning many chemical features.

Melia and Bowman (88)

Melia and Bowman have treated the coal as retaining a well-defined pore structure throughout pyrolysis, but allow for the swelling of the pores during the period when coal shows a softened character. There is no attempt made to explain the variation of pyrolysis yields with pressure. This is mainly a pseudo-kinetic model of pyrolysis with a hypothesized swelling mechanism superimposed. The general structure of the pyrolysis model is as shown:

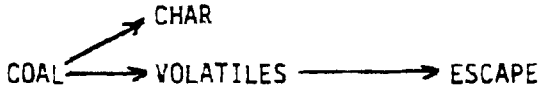

No attempt has been made to distinguish between different kinds of volatiles, and a single molecular weight was assumed for all species. The release of volatile species is assumed to be governed by a Gaussian-type distributed activation energy model, as developed by Anthony et al. (17).

Transport within the particles is modeled using an equation normally employed in analysis of flow in packed beds (and which in turn was derived by analogy with flow in parallel capillaries):

$$\Delta P = KR^a D^b T(m/n)^c/(1 + \Delta P/2) \quad (14)$$

where m is the mass rate of volatiles evolution as governed by chemical kinetics, n is the number of pores through which flow occurs, T is temperature, R is particle radius (assumed proportional to pore length), D is the pore diameter, ΔP is the particle center to surface pressure drop, and K,a,b and c are all adjustable parameters. The swelling of the particle is governed by the magnitude of the calculated pressure drop, and is governed by:

$$\Delta L/L = 3\,\Delta P\,\Delta t/8 \quad (15)$$

where L represents any characteristic dimension of the particle (i.e. diameter), μ is the coal melt viscosity, and t is time. Swelling ratios between 1 and 10 were predicted, if a softening temperature of 850 K, a resolidification temperature of 1050 K and a viscosity of softened coal of 10^6 poise were assumed. A distributed activation energy model was used to describe the rate of volatiles release (17), with mean activation energy of 62.1 kcal/mol and preexponential of 10^{14} sec^{-1}.

Again, this model depends upon a large number of adjustable parameters which cannot be experimentally verified independently of the system in question. It is also questionable whether the postulated physical picture of pore swelling would be realistic in a highly fluid coal.

Oh et al. (89-91)

This very recently presented model combines some of the features of the evaporation/diffusion models (to be presented in the next section) with some new approaches to the problem of modeling bubble dynamics and particle swelling. It, of course, again applies only to softening coals. Here, only the parts of the model which apply to bubble dynamics and swelling are considered.

It is assumed that bubbles are uniformly distributed throughout the softened coal. C_j is the number concentration of bubbles containing j molecules of vapor (mostly fixed gases). There is no restriction on the smallest size of a bubble; C_1 represents a single molecule in solution. The growth of bubbles by molecular diffusion involves a process symbolized by:

$$C_1 + C_j \longrightarrow C_{j+1} \quad (16)$$

with a rate given by

$$K_j = 4\pi r_j^2 h(C_{eq}-C_1)/C_1 \quad (17)$$

where r_j is the radius of a bubble containing j molecules, h is the mass transfer constant and C_{eq} is the equilibrium solubility of the gas in the coal melt. Thus growth of a bubble by diffusion through the coal melt is proportional to bubble surface area (as assumed by Lewellen (56)) and to the degree of supersaturation of the coal melt. The coalescence is modeled by a process:

$$C_i + C_j \longrightarrow C_{i+j} \quad (18)$$

where the rate is given by:

$$P_{ij} = 4\pi(r_i+r_j)^2(dr_i/dt + dr_j/dt) \quad (19)$$

where the time derivatives of the bubble radii (i.e. growth rates) are given by Eq. 13. The bubble conservation equations are:

$$dC_1/dt = Q_c - C_1 \sum_{i=2}^{N} K_i C_i - E_1 \qquad (20)$$

and

$$dC_j/dt = K_{j-i}C_{j-i}C_i - K_jC_jC_1 + 1/2 \sum_{i=2}^{j-2} P_{i,j-i}C_iC_{j-i} - \sum_{i=2}^{N} P_{ij}C_iC_j - E_jC_j \qquad (21)$$

where Q_c represents the rate of production of volatiles within the coal melt, and E_j represents the rate of escape of bubbles of size j from the particle surface:

$$E_j = 3(R_p - r_j)^2(da_j/dt)/R_{po}^3 \qquad (22)$$

where R_p is the radius of the coal particle (R_{po} refers to the initial radius)

In this work, the viscosity of the coal melt was taken as:

$$\mu = C_v \exp(E_u/RT)\ f(\beta) \qquad (23)$$

where C_v is a constant, E_u = 45.5 kcal/mol, and β is the fraction of metaplast in the coal melt. An equation for $f(\beta)$ was derived on the basis that a molten coal particle is a heavily solids-laden fluid, for which it can be shown that, as $\beta \rightarrow 0$,

$$f(\beta) = K/\beta \qquad (24)$$

where K is a constant. The values of C_v and K were adjusted so as to give $\mu = 10^4$ poise at heating rates of hundreds of degrees per second and a temperature of 773 K, in line with the results of Fong (53). The surface tension was taken as constant in this study, based on the results of Pelofsky (92), which show that the surface tension of high viscosity liquids is nearly constant (i.e. independent of viscosity). A value of 30 dyne/cm was assumed, based on literature values for coal liquids (93).

The model has been mainly applied to prediction of product yields thus far, based on a model of tar cracking in both liquid and bubbles. Results of the model for prediction of swelling behavior have not been presented, except in a few cases. The swelling ratios, based in particle diameter, appear to be in the range of 3 to 6, in line with some earlier reported measurements in inert gas (70). Predictions of product composition histories (for heated mesh type experiments) are also reasonable, if the following first order kinetic constants are assumed:

Process	E (kcal/mol)	A (sec^{-1})
Gas formation	26.8	10^{13}
Metaplast formation	21.7	2.9×10^6
Metaplast decomp. (liq)	18.8	3.0×10^5
Metaplast decomp. (bubbles) (94)	15.4	10^3

The metaplast decomposition parameters are quite different than those for metaplast decomposition reported by Fong et al. (52), i.e. E = 42.2 kcal/mol and A = 1.9×10^{10} sec^{-1}. These latter values are in fair comparison with the range reported some time ago by Bronowski et al. for "carbonization" (47.3 to 52.7 kcal/mol) (95).

The disagreement in these values warrants further attention.

General Features of Evaporation-Diffusion Control Models

These models view diffusion in the gas phase above the surface of the coal as limiting the rate of transport of tar away from the particle. The assumption of a well-mixed, softened coal particle has usually been employed. At present, several models which account for internal transport limitations are under development. The considerations inherent in treating a softened particle as well-mixed were previously outlined in Section 4.1. All of the following models assume the particles to be spatially isothermal, of course allowing for temporal variations of temperature. The assumption is also made that continuum diffusion theory can be applied in the gas phase surrounding the particles. This is probably questionable under vacuum conditions, but this issue has not been addressed in any coal pyrolysis modeling work.

The equations presented below are derived for the case of spherically symmetric particles, but the case of a flat plate geometry will be mentioned later.

The rigorous starting point for a multi-component gas mixture diffusion problem is the Stefan-Maxwell equation (96):

$$\nabla y_i = \sum_{j=1}^{n+1} (1/C_v D_{ij}) (y_i N_j - y_j N_i) \qquad (25)$$

where, as usual, Y_i represents a mole fraction and N_i a molar flux of i. the total number of species diffusing from the particle is n, and component n+1 is the inert gas surrounding the particle. It is difficult to use this generalized form for actual solution. Normally the assumption is made that the diffusivity of species i relative to any species j in the mixture is a constant, i.e. $D_{ij} = D_i$. Often the further assumption is made that all D_i are equal, but here this assumption will be put off for the moment. The simplifying assumption concerning the diffusion coefficients allows expressing species fluxes in a form analagous to Fick's Law in a stationary coordinate system:

$$N_i = y_i \left(\sum_{j=1}^{n+1} N_j\right) - C_v D_i (dy_i/dr) \qquad (26)$$

It is now explicitly assumed that the concentration gradients exist only in a radial direction.

In deriving the species continuity equations for the vapor surrounding the particle, it is normally assumed that pseudo-steady state exists, because the time scale for adjustment of gradients is short compared to the characteristic time scale for pyrolysis. Since no source or sink terms exist in the vapor phase, the species continuity equation is particularly straightforward to integrate, giving:

$$r^2 N_i = R^2 N_{io} \qquad (27)$$

where N_{io} is the flux of i at the particle surface (r = R). Solving for N_i in Eq. 27 and substituting this result into Eq. 26 yields an easily integrable equation. The boundary conditions for integration of the n+1 resulting equations are that all y_i (except y_{n+1}) are zero at infinite distance from the particle. In addition, $y_{n+1} = 1$, since the particle is surrounded by inert gas. At the particle surface itself, Raoult's Law is usually assumed to hold, such that:

$$y_i = y_{io} = x_i P_i^o / P_{tot} \qquad (28)$$

where x_i is the mole fraction of i in the condensed phase at the particle surface, P_i^o is the pure component i vapor pressure, and P_{tot} is the total atmospheric pressure. Integration of Eq. 26 yields after some manipulation:

$$N_{io} = N_{to}\left[\frac{y_{io}\exp(N_{to}R/C_vD_i)}{\exp(N_{to}R/C_vD_i) - 1}\right] \tag{29}$$

for all i except i=n+1 (the inert gas). Where $N_{to} = \sum_{j=1}^{n+1} N_{jo}$. For the inert gas:

$$N_{n+1,0} = 0 = N_{to}\left[\frac{y_{n+1,0}\exp(N_{to}R/C_vD_{n+1}) - 1}{\exp(N_{to}R/C_vD_{n+1}) - 1}\right] \tag{30}$$

where it is recognized that inert gas is neither created nor destroyed. Equation 30 may be solved for N_{to}, and $y_{n+1,o}$ eliminated. Hence:

$$N_{to} = +(C_vD_i/R)\ln(1/y_{n+1,o}) = -(C_vD_i/R)\ln(1-\sum_{i=1}^{n} y_{io}) \tag{31}$$

Substitution of this expression for N_{to} into Eq. 29 permits solving for the flux of i from:

$$N_{io} = \frac{C_vD_{n+1}}{R}\ln(u)\left[\frac{y_{io}u^{q_i}}{u^{q_i} - 1}\right] \tag{32}$$

where $q_i = D_{n+1}/D_i$ and $u = (1-\sum_{i=1}^{n} y_{io})^{-1}$.

The solution assumes a somewhat simpler form if all vapor species are all assumed to have similar diffusivities (probably a fair assumption); thus $q_i = 1$. If it is further assumed that the tar is relatively non-volatile, such that $\sum_{i=1}^{n} y_{io} << 1$, then a very simple result emerges:

$$N_{io} = C_vD_{eff}x_iP_i^o/RP_{tot} \tag{33}$$

This result was previously demonstrated by a similar line of reasoning (25). The P_i^o are provided by Eq. 3, and the x_i are known from the molecular weight distribution of the metaplast.

Finally, consider the effect of a superimposed gas product flux on this result. Consider the gaseous pyrolytic products (exclusive of tars) to be the component n, whose flux ($N_{no} = N_g$) is determined solely by reaction kinetics (i.e. there is no need to consider vapor-liquid equilibrium). Assuming $q_g = 1$, then:

$$N_g = \frac{C_vD_g}{R}\ln(u)\left[\frac{y_{go}u}{u-1}\right] \tag{34}$$

which is now an equation which may be used to solve for y_{go}. With this value of y_{go}, solution may now be effected using Eq. 32. As was discussed earlier in Section 3.0, the contribution of such a gas flux can be quite significant when particles exceed a few hundred micrometers in size. Equation 32 and/or 33 will be considered the primary working equations in the models below.

Suuberg et al. (6)

This model pertains specifically to softening coals. The general structure of the model is:

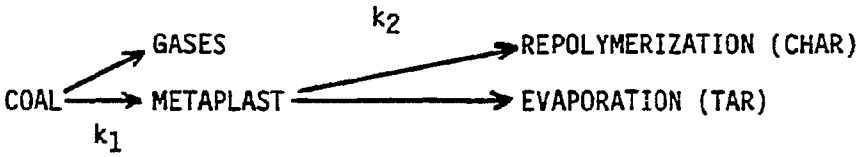

where k_1 and k_2 represent, respectively, rate constants for formation and destruction of metaplast (the as yet unevaporated tar precursors within the particle). In the implementation of this model, k_1 was determined to be characterized by an activation energy of 40 kcal/mol and a pre-exponential of $10^{13} s^{-1}$. These parameters are independently set, based on assuming that the coal to metaplast reaction must be roughly 50% complete at experimentally observed softening temperatures. They are reasonably insensitive to the percentage conversion selected, within a rather wide range. it should be noted, that these rate constants assure that the time scale for metaplast formation is short in comparison to the time scale for the remainder of the pyrolysis process, under typical conditions.

The metaplast that is formed during the initial reaction has been assumed to have molecular weights in the range 400 to 1200, with the shape of the distribution an adjustable quantity. The vapor pressure of this material can be estimated with an equation similar to Eq. 3. The actual rate of tar evolution is calculated by use of Eq. 33. The rate of metaplast repolymerization is modeled as first order in metaplast, with the activation energy of the process determined as roughly 65 kcal/mol, based on the observation of temperature at which yields from vacuum and atmospheric pressure experiments diverged. Thus, k_2 is set independently of the actual pyrolysis model. Finally, the gaseous products of pyrolysis are assumed to evolve independently of the tars, at rates measured experimentally and are modeled as a series of first order processes.

Reasonable agreement has been obtained between the tar yield data of Fig. 1 and the model calculations. The key adjustable parameters which permit reasonable agreement to be achieved are the total yield of metaplast and the molecular weight of the metaplast. The following table shows a metaplast molecular weight distribution that provides a reasonable fit to the tar total mass yield data, and the resulting predicted molecular weight distribution of the tar. The results are in reasonable accord with the recently obtained data on tar molecular weight distributions shown in Fig. 4.

MW	METAPLAST	TAR
200	0	0
400	2	2
600	2	2
800	6	6
1000	10	9
1200	12	6

(all values in wt.% of coal)

Gaseous yields at atmospheric pressure are well-modeled, since a large number of adjustable parameters are employed to describe their evolution. It is unlikely that the number of such parameters can be significantly decreased, since each species evolves by a chemically distinct route. It will hopefully be possible to

eventually relate these gaseous evolution parameters to distinct chemical structures in the parent coals, and thus gain true predictive power. Such attempts are detailed below.

The observation must be made that distributed molecular weight models allow a great deal of curve-fitting flexibility within a reasonable range of molecular weights. Their use, without experimental verification of the true distribution of molecular weights may be dangerous.

Zacharias (42)

This model is quite similar in form to that discussed in the previous section. Significant efforts were made to more carefully estimate the diffusion coefficients of tars in the surrounding gas, but the effect of small variations in this parameter are unimportant.

One significant difference between this and the preceding model is in the geometry considered. Whereas the above model is concerned with the behavior of isolated, spherical particles, the present model has been derived to describe pyrolysis in a heated wire mesh experimental apparatus. In this system, the coal approximates a thin flat slab, rather than individual spherical particles. The flux from the surface of the slab is given by:

$$N_{io} = 2C_v D_i P_i^o x_i / P_{tot} \quad \delta m \qquad (35)$$

where δm is a diffusion film thickness calculated from boundary layer theory and a knowledge of the flow pattern around the wire mesh which confines the coal "slab".

Small differences also exist in the treatment of the metaplast formation reaction kinetics, the metaplast decomposition reactions and the shape of the metaplast molecular weight distribution. The metaplast formation reactions are, in this case, modeled as being characterized by a distribution of activation energies. This is considerably more realistic than requiring a single activation energy to characterize the depolymerization process. Undoubtedly there are many types of bonds which can be cleaved to give the tar precursors.

The model also allows for the formation of gases from decomposition of metaplast which has not escaped the particles. This is likewise realistic. Since the metaplast is quite similar to the parent coal, it should be able to undergo the same sorts of reactions. By the same token, if metaplast does escape the particle, it is no longer available for participation in gas forming reactions and the gas forming tendency of the coal is reduced (see Fig. 1 and relevant discussion in Section 2.0).

The distribution of metaplast molecular weights needed to achieve a good fit to the temperature and pressure trends of tar yields is reasonable. The mean is in the range of 560 to 580, with a standard deviation of about 150 to 250, for the Pittsburgh high volatile coal considered. These values are low when compared to the extract molecular weight distributions in Fig. 4, but compare favorably with the actual atmospheric pressure tar molecular weight distributions.

Urger and Suuberg (25)

The structure of this model is quite similar to the two which have preceded it. once again, a spherical particle is assumed.

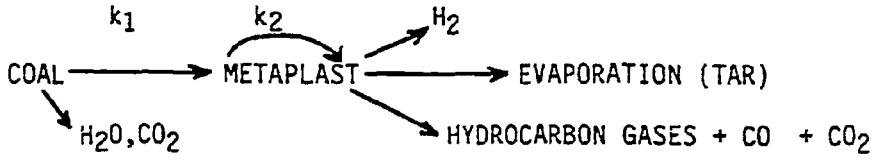

The major difference between this and the earlier versions of this type of model are in details of the chemistry. The very important role of donor hydrogen has been highlighted. Another key difference between this and the earlier models of this kind involves an attempt to avoid arbitrary specification of what fraction of coal can form metaplast. In the present implementation, all of the reactive (i.e., except ash, inertinite) portions of the coal are assumed to form metaplast at a rate given by k_1 (the rate parameters were determined as outlined in Ref. 6). The metaplast so formed is governed by a Gaussian molecular weight distribution, the mean and standard deviation of which remain adjustable parameters.

Once formed, the metaplast species participate in what are assumed to be irreversible repolymerization reactions to yield high molecular species. This rate (k_2) is tied to the aromatization process, which evolves hydrogen. The increase in molecular weight which accompanies these repolymerization processes decreases the fraction of potentially volatile metaplast. This treatment is quite different than those in the earlier models. It is assumed that metaplast does not go to char in a single step, but that it reacts in a gradual polymerization process to form progressively higher molecular weight material.

The shuttling of hydrogen between various chemical groups occurs as a result of several processes. Aliphatic hydrogen is consumed whenever a bond breaks to form a metaplast species. Likewise, aliphatic hydrogen is lost via evolution of hydrocarbon gas species. All forms of hydrogen are carried away by the tars, in proportion to their amounts in the particle at any time. This permits predictions of hydrogen to carbon ratios to be made throughout the pyrolysis process. The ratios of the different types of hydrogen within the tars appear to agree reasonably with what few data are available, but the model requires further validation on this point.

A reasonable fit to atmospheric pressure tar yield vs temperature data is achieved by assuming the metaplast to be formed with an initial mean molecular weight of 1200 and a standard deviation of 360 g/mol. The agreement between this mean value and the actual peak of the extract curves shown in Fig. 4 is reasonable. It is, however, felt that the model results are unrealistic in the sense that at no time does the coal become 100% extractable as is predicted. If the molecular weight of the whole coal were to decrease as quickly as postulated to the values suggested above, complete extractability might be expected at temperatures near the softening temperature. Nevertheless, Fong et al. (52) have shown extractability of nearly 80%, which confirms the high degree of breakdown of the macromolecular structure.

Not surprisingly, the model considerably overpredicts yields at vacuum conditions, since internal transport limitations are not included. This sort of overprediction at vacuum is not observed with the two previously discussed models because they both involve treating the maximum yield of metaplast as an adjustable parameter. Both previous models permit only about 1/3 of the coal to form transportable metaplast. In actuality, such a parameter would take into account the fact that metaplast formed deep within the particle cannot escape. The weakness of such an approach is that this fraction is not a-priori predictable. See the next model for further discussion of this point.

The activation energies for metaplast formation and retrograde reactions are 40 kcal/mol and 65 kcal/mol, respectively. This, again, highlights the fact that

there exists a significant spread of values for these parameters in the different pyrolysis models, and this is an issue requiring settling before any models are considered "reliable".

Suuberg and Sezen (97)

This study was undertaken to establish whether softening coal pyrolysis models, which postulate **internal** transport by liquid phase diffusion, could predict the major observed trends quantitatively correctly given "reasonable parameters" for describing the kinetic and transport processes in such coals. There was concern that the assumption of bubble-phase-transport-control of volatiles escape was perhaps unnecessary. Consequently, the external diffusion control model developed by Unger and Suuberg (25) was combined with a model of internal diffusion of metaplast species, governed by

$$\frac{D_L}{r^2}\frac{\partial}{\partial r}\left(r^2\frac{\partial w_i}{\partial r}\right)+\frac{\phi_i}{\rho_L}=\frac{\partial w_i}{\partial t} \qquad (36)$$

where D_L is the diffusivity of metaplast species in the particle, W_i is the mass fraction of metaplast species of molecular weight M_i at any radial position r in the particle, ρ_L is the density of the particle, and ϕ_i is a net volumetric production rate of metaplast species i, involving both formation and retrograde reactions.

Reasonable fit was obtained to the data of Figs. 4 and 9 if the value of D_L was 5×10^{-6} cm^2/s, the metaplast formation activation energy is 35 kcal/mol, and the activation energy for retrograde reactions is 60 kcal/mol.

The sensitivity of the model to particle diameter and diffusion coefficient is large, and being re-examined. But at least the tentative conclusion is that there is not necessarily a need to invoke transport of tars out of the particles by bubbles, in order to correctly predict trends. This should not be misconstrued as a suggestion that bubble transport models are not important, but rather than their development should proceed together with classic diffusion models.

Solomon et al (10,34-36,98,99)

This model constitutes the cornerstone of further model developing on this project. What is offered here is a cursory historical perspective on its development. In the early versions of this model, the emphasis was mainly on the chemistry of pyrolysis rather than on the mass transfer aspects of the process (10). Transport of tar was only indirectly considered via psuedo-chemical rate parameters which included tar evaporation. These parameters did not account for any pressure or particle diameter effects. The general structure of the early pyrolysis model was:

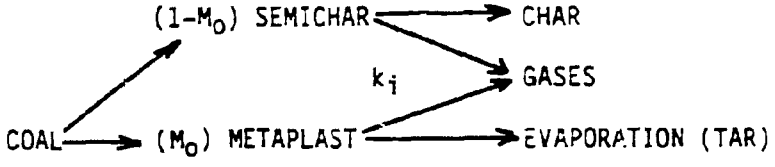

The term metaplast has been introduced here for consistency with discussions of the previous models. In the original presentation of this model, the term "potential tar forming fraction" was used instead. The use of the term metaplast here should not connote any softening tendency, since this model has been applied to softening and non-softening coals alike. Likewise, there term semichar has been substituted

for the term "non-tar-forming fraction", and indicates a fraction which will not lead to tar.

The fundamental structure of this model is thus quite similar to several of the other models discussed to this point. It is important to note that this model placed a great deal of emphasis on correct prediction of light gaseous species evolution. The prediction of how much of a particular gas can be evolved was largely based on empiricism, but a concerted effort was made to tie these predictions to a knowledge of the starting structures within the coal (as revealed by a combination of elemental analysis and infrared spectroscopy).

The gaseous species could evolve either from the semichar fraction or the metaplast, with the same kinetics. The only distinction to be drawn between these two sources it that the metaplast may escape as tar before it can react, thus carrying away a certain fraction of the structures which would otherwise be able to form light gases. The model can be viewed in the following terms.

It is assumed that there is an initial pool of metaplast, consisting of M_o "molecules". The rate of metaplast molecule disappearance (via bond rupture and evaporation) is assumed to be first order in the number of molecules (M) in the pool at any time:

$$dM/dt = -k_t M \tag{37}$$

or, integrating over time:

$$M = M_o \exp(-k_t t) \tag{38}$$

It was assumed that the particle is isothermal over its lifetime, but allowing for non-isothermality is straightforward. There was in this early model no allowance for repolymerization reactions of the metaplast. Once one of these molecules of metaplast is produced, its only possible fate is to escape the particle, as demanded by Eq. 38. The molecular mass of metaplast "molecules" can, however, be decreased by the loss of sidegroups which form the light gases. The loss of any sidegroup i by cracking reactions is also modeled by a first order process

$$dm_i/dt = -k_i m_i \tag{39}$$

where m_i is the mass of i remaining in the semichar plus metaplast. The problem of modeling the pyrolysis reduces to one of bookkeeping, wherein proper account must be taken of i lost by chemical reaction,vs. release and evaporation with the tar. The groups i are equally distributed throughout the semichar and metaplast.

Further development of the gas release model involved noting that to a first approximation, all coals release the same gaseous species (in different proportions) with the same kinetics (98,99). It was also noted, as has been shown before (100-104), that rather than being able to describe the release of each gaseous species in terms of discrete, single reaction kinetics, a Gaussian distribution of activation energies was required for each species (98,99). The current set of constants for the major gas species is shown in Table III.

It is to be noted that tars are singled out for special attention in Table III. While a set of pseudo rate parameters is offered for tar evolution, it is clear from the preceding discussion in this section that tar release can not be modeled as a simple chemical process. Based upon: 1. the observation that tar molecules appear to be fragments of the present coal (20-23), 2. the success of vaporization rate limited models in describing several features of tar release (6,15,17,25), and 3. new insights into the macromolecular structure of coal e.g., Ref. 105, a new

TABLE III

Universal Kinetic Rate Constants for Gas Release During Pyrolysis

$k_i = k_{io} \exp(-(E_o/R + \sigma/R)/T)$

CO_2 extra loose	$k_1 = 0.56E{+}18 \exp(-30000 \pm 2000)/T)$
CO_2 loose	$k_2 = 0.65E{+}17 \exp(-33850 \pm 1500)/T)$
CO_2 tight	$k_3 = 0.11E{+}16 \exp(-38315 \pm 2000)/T)$
H_2O loose	$k_4 = 0.22E{+}19 \exp(-30000 \pm 1500)/T)$
H_2O tight	$k_5 = 0.17E{+}14 \exp(-32700 \pm 1500)/T)$
CO ether loose	$k_6 = 0.14E{+}19 \exp(-40000 \pm 6000)/T)$
CO ether tight	$k_7 = 0.15E{+}16 \exp(-40500 \pm 1500)/T)$
HCN loose	$k_8 = 0.17E{+}14 \exp(-30000 \pm 1500)/T)$
HCN tight	$k_9 = 0.69E{+}13 \exp(-42500 \pm 4750)/T)$
NH_3	$k_{10} = 0.12E{+}13 \exp(-27300 \pm 3000)/T)$
CH_2 aliphatic	$k_{11} = 0.84E{+}15 \exp(-30000 \pm 1500)/T)$
methane extra loose	$k_{12} = 0.84E{+}15 \exp(-30000 \pm 1500)/T)$
methane loose	$k_{13} = 0.75E{+}14 \exp(-30000 \pm 2000)/T)$
methane tight	$k_{14} = 0.34E{+}12 \exp(-30000 \pm 2000)/T)$
H aromatic	$k_{15} = 0.10E{+}15 \exp(-40500 \pm 6000)/T)$
methanol	$k_{16} = 0.00E{+}00 \exp(-30000 \pm 0)/T)$
CO extra tight	$k_{17} = 0.20E{+}14 \exp(-45500 \pm 1500)/T)$
C nonvolatile	$k_{18} = 0$
S organic	

Tar $\quad k_t = 0.45E + 14 \exp(-(26400. + 1500.)/T)$

E_o = mean activation energy

σ = standard deviation of activiation energy

Serio, et al., Energy & Fuel, 1, 138, (1987).

model of coal fragmentation, crosslinking and tar volatilization was developed (34-36). Considerable use was made of polymer model compounds in constructing the elements of the theory. The vaporization theory is largely that described earlier (25), while the depolymerization reactions are modeled in a manner similar to that proposed by Gavalas et al. (106). It has been noted here, as earlier (25), that donatable hydrogen correlates to some extent with tar yield (107) which led to the incorporation of a mechanism stressing hydrogen capping of radicals into this model.

The final element in development of this model for softening coals is the inclusion of a swelling submodel. The model (98) is, in considering the growth of bubbles, similar to those employed by Lewellen (56) and later Oh (89-91). The bubble is considered spherically symmetrical with respect to the particle, and surface tension effects are neglected in determining growth rate. A rupture criterion is defined as

$$P_c = -P_2 + \frac{1.5\, r_1^3\, (P_1 - P_2)}{r_2^3 - r_1^3} \qquad (40)$$

where P_c is a critical stress, P_2 is the external pressure, r_2 is the particle radius, r_1, is the bubble radius and P its pressure.

For an assumed viscosity of the softened coal of 1×10^4 poise and a critical stress of P_c = 10 atm, the particle swelling behavior was very realistic, and the internal particle pressures were somewhat more realistic than those obtained by Lewellen (56). The objective will be to tie the viscosity of the coal melt in with the depolymerization model discussed above.

4.2 Non-Softening Coals

The transport of species within coals which do not soften must largely be governed by transport within the pore structure of the coals. There exist many reviews on the nature of porosity in coals (e.g. 45,108-110). The porosity of coals is divided according to the normal conventions employed for most porous solids; macropores are pores with diameters greater than about 300Å (500Å) and less than 5 to 10 μm, micropores are smaller than about 12Å (20Å) in diameter, and transitional pores exist between these limits. The figures in parentheses are the IUPAC recommended values. The distribution of porosity according to these limits is shown in Table IV for a variety of coals (111).

It is apparent from the data in Table IV that the coals displaying significant amounts of transitional porosity are just those which will tend to soften during pyrolysis (the high volatile bituminous ranks). There are certainly a few exceptions. Anthracites apparently show a significant amount of transitional porosity, but are of little interest here because they yield very little tar during pyrolysis. In one case (13), a subbituminous coal showed a significant amount of transitional porosity. Except for such materials, it might be reasonable to assume that the porosity exists only as macro- and macro-pores for the purposes of modeling transport during pyrolysis.

The changes in pore structure occurring during pyrolysis have been studied to a limited extent in the case of non-softening coals. It has been observed in one case that little formation of what can be interpreted as transitional porosity occurs during pyrolysis (112). In general, total porosity increases with extent of pyrolysis, but accessibility of porosity to large molecules can decrease (45).

Typically, apparent porosity may increase from an initial value of 10% to a final value of 50% during pyrolysis. The helium density of the coal solid is not

TABLE IV

Pore Size Distributions for Various Ranks of Coal[a]

Sample	Rank	V_T[b] (cm^3/g)	V_1[c] (cm^3/g)	V_2[d] (cm^3/g)	V_3[e] (cm^3/g)	V_3(%)	V_2(%)	V_1(%)
PSOC-80	Anthracite	0.076	0.0009	0.010	0.057	75.0	13.1	11.9
PSOC-127	LVB	0.052	0.014	0.000	0.038	73.0	0	27.0
PSOC-135	MVB	0.042	0.016	0.000	0.026	61.9	0	38.1
PSOC-4	HVA bituminous	0.033	0.017	0.000	0.016	48.5	0	51.5
PSOC-105A	HVB bituminous	0.144	0.036	0.065	0.043	29.9	45.1	25.0
Rand	HVC bituminous	0.083	0.017	0.027	0.039	47.0	32.5	20.5
PROC-26	HVC bituminous	0.158	0.031	0.061	0.066	41.8	38.6	19.6
POC-197	HVB bituminous	0.105	0.022	0.013	0.070	66.7	12.4	20.9
PSOC-190	HCV bituminous	0.232	0.040	0.122	0.070	30.2	52.6	17.2
PSOC-141	Lignite	0.114	0.088	0.004	0.022	19.3	3.5	77.2
PSOC-87	Lignite	0.105	0.062	0.000	0.043	40.9	0	59.1
PSOC-89	Lignite	0.073	0.064	0.000	0.009	12.3	0	87.7

[a] Reference 111.
[b] V_T = total porosity.
[c] V_1 = Macroporosity (300 Å-1 μm).
[d] V_2 = transitional porosity (12-300 Å).
[e] V_3 = microporosity (4-12 Å).

constant during such a process, and may vary from around 1.3-1.4g/cc to about 1.8-2.0g/cc during pyrolysis (113). Various correlations exist which may allow calculation of helium densities from elemental composition (114).

When focussing specifically on the variation of surface area in rapidly heated coals, the data are somewhat more limited. Nsakala et al. (115) have shown that the helium density, CO_2 surface area, and N_2 surface area increased by varying amounts in rapidly heated lignites, during the first 30% weight loss. In one case, the CO_2 area changed less than 10%, whereas in another type of lignite the increase was from $200m^2/g$ to over $300m^2/g$. N_2 surface areas generally paralleled these trends, but were generally considerably lower. Similar trends were noted in a study on medium and low rank U.K. coals, in air (116). In fact, after devolatilization was complete, the xenon surface areas (comparable to CO_2) of chars were noted to decrease with increasing time in the furnace. Recently, another study (117) of surface areas of chars produced in inert gas by rapid heating revealed that the CO_2 surface area of a lignite increased rapidly with devolatilization in the range of temperatures 1000 to 1300°C. The micro pore radii were largely unchanged under these conditions. There was a slight indication that the surface area increase was smaller with increasing temperature of devolatilization. A subbituminous coal showed a similar pattern. A softening high volatile bituminous coal showed the most dramatic behavior of this sort, giving the results shown below.

Temperature	% Weight Loss	Surface Area (m^2/g)
1000	46.3	401
1100	53.4	304
1200	52.3	109
1300	59.0	21

These results are in quantitative agreement with the results of a study on chars prepared in nitrogen fluidized beds (118). A lignite showed a rather dramatic opening of CO_2 porosity during pyrolysis, but the value of surface area decreased slightly with increased temperature of pyrolysis. A high volatile A bituminous coal showed a large increase in surface area during pyrolysis, and a significant decrease in this quantity with increased temperature of heat treatment. More interesting was the fact that the N_2 surface area of the lignite increased dramatically in pyrolysis, and decreased just as dramatically during heat treatment. The high volatile A bituminous coal showed very little N_2 surface area under any conditions.

It appears that charges in the pore structure of rapidly heated coals are significant and, because of their complicated behavior, may be difficult to predict a-priori. This area certainly warrants more attention.

4.2.1 Significance of Porous Structure on Tar Transport During Pyrolysis

Since microporosity is of a scale comparable to the dimensions of the diffusing tar species (of order 1 to 10Å), it is likely that there will be strong pore wall/tar molecule interactions. As a result, diffusion in such a case is likely to be activated, and that prediction of diffusivity will be as difficult as in a true condensed phase. Such diffusion is sometimes termed hindered diffusion or configurational diffusion.

When the mean free path of the diffusing species is long compared to the dimensions of a pore, but wall-molecule interactions are limited to collisional precesses, Knudsen diffusion will control transport. This is likely to be the case for light gas molecules in micro- and transitional pores, and perhaps for tar molecules in transitional pores. At atmospheric pressure and temperature, small gases typically

exhibit mean free paths of order 1000Å (varying inversely with molar density). As a result, Knudsen diffusion may be important in small pores even if the pressure in the pore in substantially above atmospheric.

Walker has shown that with increasing extent of gasification, the opening up of the pore structure occurs to an extent that micropores which initially allowed only activated diffusion, become "open" enough to permit Knudsen diffusion (119). The data were for diffusion of methane in anthracite chars, but there is no reason to believe that the same processes are not important for other species in other chars.

Inasmuch as the focus here for the moment is on the transport of tar molecules, issues of transport in micropores will be disregarded. Instead, it will be assumed that a condensed phase diffusional transport process is responsible for carrying the tars from the bulk of the pyrolyzing coal into the macropores. At the surface of the macropores, it is likely that a vapor-liquid equilibrium will exist, just as discussed in the context of the softening coal models. This simplified picture is similar to one suggested in a recent study, in which an empirical coefficient was used to describe the fraction of tar which reached the macropore wall (106).

Transport within macropores can occur by either a diffusional or convective mechanism. It has been noted that for atmospheric pressure and below, both mechanisms can be important, whereas at higher pressures, convection almost certainly dominates (4,120). This can be shown by a comparison of characteristic times for transport by diffusion compared to convection (120):

$$t_{diff}/t_{conv} = PB/\mu D_{eff} \qquad (41)$$

where D_{eff} is the effective diffusivity of vapor through the particle, B is the permeability of the particle, μ = viscosity, P = pressure, and R = particle radius. Assume that $D_{eff} = De/\tau = O(10^{-1}$sq cm/sec), where e = voidage (order 10^{-1}), τ = tortuosity (order unity); μ = order (10^{-4}g/sec-cm), and $B = r^2e/24 = O(r^2 \times 10^{-2})$, where it is assumed that the pores are straight cylinders of radius r. Thus:

$$t_{diff}/t_{conv} = Pr^2 \times 10^3 \qquad (42)$$

if P=1 atm (=1 x 10^6g/sec^2-cm), and the macropores are characterized by a radius of 1000Å (=10^{-5}cm), then diffusion dominates. In larger pores (e.g. 1 μm = 10^{-4}cm), the time scales are comparable. Consequently, the equations used to describe pore transport are written to include both diffusional and convective transport.

Simple geometric arguments suggest that the distance which a species would have to diffuse through micropores to reach a macropore would be:

$$X = r\left[(1/e)^2-1\right] = rK \qquad (43)$$

This assumes that the coal is uniformly distributed around cylindrical pores of radius r. On this basis, the ratio of characteristic times for micropore diffusion to macropore diffusion would be:

$$t_{micro}/t_{macro} = (D_{macro}/D_{micro})K^2(r/R)^2 \qquad (44)$$

where K is normally of order 10 to 10^2, (r/R) would be of order 10^{-3} to 10^{-2} for typical macropores and a particle radius R of 100 μm; the ratio of diffusion coefficients is unknown because D_{micro} is unknown. It is however apparent that if D_{micro} is of the same magnitude at the previously discussed liquid diffusivities, micropore transport will actually be a more significant limitation to escape of tar than macropore transport. On the other hand, if the ratio of the diffusion coefficients is near unity, macropore transport will undoubtedly control.

The effect of increasing pressure on tar yield is most likely felt through the increase in residence times of tar in pores. If diffusion controls transport and the diffusional process is Fickian (rather than Knudsen), then the effect of pressure can be seen through the inverse pressure dependence of the diffusional coefficient. Pure Knudsen diffusion control would not exhibit any pressure dependence. If convection in macropores controls transport, then the rate of tar escape will depend in a complex way on pressure. This will be apparent in the next section, which deals with details of the transport models.

4.2.2 Modeling of Non-softening Coal Pyrolysis

Obviously the description of transport in porous coal particle exhibits strong analogies to many other porous solid models.

All three porous transport models assume spherical particles of constant radius, although one employs a pseudo-radius rather than a true radius. In all cases, it is assumed that the inventory of vapor phase volatiles within the pores is sufficiently small so that the time derivative of any vapor phase species concentration within the particle may be taken as zero. As a result, the general species i conservation equation within the particle may be written as:

$$(1/r^2)d/dr(r^2N_i) = R_i \qquad (45)$$

where r is the radial position within the particle, N_i is a molar flux of i at any radial position, and R_i is the production rate of i per unit volume of particle. This equation of course may be changed over to a mass basis merely by multiplication by the molecular weight of i, and is so expressed in some treatments.

Typically, some sort of ternary mixture approximation is made for the vapors within the particle. Thus i can represent tars (or "reactive volatiles"), fixed-gases (or "non-reactive volatiles"), or the inert gas which surrounds the particle (for which case R_i=0). If it is possible to assume that the rate of production and/or destruction of tars and fixed gases is independent of position and vapor phase concentrations, then the integration of Eq. 45 is straightforward and yields:

$$N_i = rR_i/3 \qquad (46)$$

It was also assumed in obtaining Eq. 46 that symmetry exists at r=0. Of course, the assumption that the rate of repolymerization of tars is independent of the vapor phase concentration of tars is felt by some to be unrealistic. Likewise, some feel that fixed gaseous volatiles are produced by tar cracking reactions, and thus the rate of gas evolution depends upon local tar concentrations. If the rate of repolymerization of tar or formation of fixed gaseous species is taken to be a function of tar concentration, then R_i for both gas and tar species will certainly be a function of r and a simple integration of Eq. 45 is no longer possible.

The main difference between the various pore transport models concerns the relation between the fluxes N_i and the actual species concentrations. Some view the diffusion as Fickian, with appropriate accounting for bulk flow, while others allow for the contribution of Knudsen diffusion mechanisms. These differences will now be outlined.

Russel et al. (120)

This model naturally pertains only to non-softening coals. The general structure of the model is as shown:

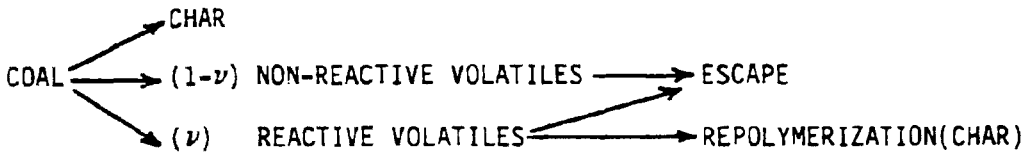

The transport limitation in this case was assumed to exist strictly within the particle. The flux of any species i within the pore system was assumed to be given by Fick's Law written for a stationary frame of reference:

$$N_i = y_i(N_r + N_{nr}) - (PD_{eff}/R_gT)dy_i/dr \qquad (47)$$

where y_i refers to the vapor phase mole fraction of i, all species are assumed to have equal diffusivities D_{eff}, and the subscripts r and nr refer to reactive and non-reactive volatiles. Note that the product of pressure and diffusivity is constant throughout the particle. It was assumed that the y_i for reactive and non-reactive volatiles were zero at the outside edge of the particles. The solution of the three coupled transport Eq. 45 with the three flux definitions Eq. 47 is not difficult despite the fact that the rate of reactive volatiles destruction (tar repolymerization) is assumed to be proportional to the local reactive volatiles concentration:

$$R_r = k_0C_c\,\nu - k_1C_vy_r \qquad (48)$$

where C_v and C_c are vapor and coal molar densities within the particle. The first term represents the formation of reactive volatiles from the coal and the second term the destruction of the reactive volatiles (see reaction scheme above). The rate of non-reactive volatiles evolution per unit volume is taken as a constant (R_{nr}), and thus Eq. 45 may be solved directly for N_{nr}:

$$N_{nr} = rR_{nr}/r^3 = k_0C_c(1-\nu)r/3 \qquad (49)$$

This may now be substituted for N_{nr} in Eq. 47, which may then be solved for N_r. The expression of N_r may then be used in Eq. 45 to solve for y_r, since the latter becomes an ordinary differential equation for y_r in terms of radial position. In one particular case, it was assumed that bulk flow dominates diffusion, so that the term involving the concentration gradient in Eq. 47 becomes small, thus:

$$N_r = y_r(N_r + N_{nr}) \qquad (50)$$

The solution for y_r with position is obtained by solving Eq. 50 for N_r, substituting Eq. 49 for N_{nr}, and substituting the resulting expression for N_r into Eq. 45. If the solution of y_r with position is further integrated over the entire particle to yield an average concentration of reactive volatiles, the result is:

$$\bar{y}_r = \frac{1+g}{2g}\left\{1 - \left[1 - \frac{4\nu g}{(1+g)^2}\right]^{1/2}\right\} \qquad (51)$$

where $g = k_1C_v/k_0C_c$. It is apparent that since C_v is a function of pressure, the average tar concentration within the particle depends upon pressure. It is apparent from Eq. 48 that the rate of tar deposition reactions will thus also depend upon pressure.

The above example is cited only to give a flavor for the solution process and to indicate the origin of the pressure dependence of volatile yields as predicted by

this model. Solution was also effected without assuming bulk flow domination of flow. A main strength of the presentation by Russel et al. involves extensive examination of limiting cases. The model was also further developed in order to examine hydropyrolysis situations (involving reaction of pyrolyzing coal with gaseous hydrogen); this will not be considered here.

The validation of this model involved fitting total weight loss vs. pressure data such as those shown in Fig. 1. The fit was quite reasonable in many respects, in part attributable to the existence of several adjustable parameters in the model. The major criticism of the validation attempt is that it compares a model which postulates that a well-defined pore structure exists throughout pyrolysis with data obtained on a softening coal which loses all pore structure during the most active phase of pyrolysis.

Chen and Wen (121)

This model is quite similar in structure to that explored by Russel et al. It again pertains only to non-softening coals, which retain a well-defined pore structure throughout pyrolysis. There is however a distinct difference in the chemical pathways considered here as opposed to those in the previous section. The structure of the present model is:

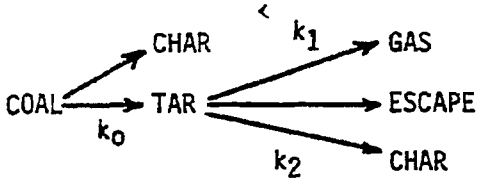

Note that the gaseous products of pyrolysis are here postulated to be secondary decomposition products of tar rather than primary products of coal decomposition. In reality, both sources are most likely to be important. The rate of tar formation/destruction is given by:

$$R_{tar} = fk_0C_c - (k_1 + k_2)C_{tar} \tag{52}$$

The rate of gas formation is given by:

$$R_{gas} = k_1C_{tar} \tag{53}$$

Again, a fixed-coordinate Fickian diffusion law is used to express the relationship between fluxes and concentration gradients, so Eq. 47 applies in this case as well. In the original formulation of this model, fluxes and concentrations were expressed in mass, rather than molar units, but the distinction is unimportant.

Solution of the problem as posed here is considerably more difficult than solution of the equations posed by Russel et al. The Eq. 45 must truly be solved simultaneously, because Eq. 53 involves a tar concentration dependence, whereas Eq. 49 did not involve a reactive volatile concentration dependence. In addition, a convective boundary condition was assumed in the present case:

$$N_i = k_{gi}(C_i - C_i) \tag{54}$$

where k_{gi} is a mass transfer coefficient for species i, and the concentration difference is taken between the particle surface (R) and the bulk (b).

Few details are given concerning the transport properties or the solution technique employed. There is no consideration of any sort of vapor-liquid equilibrium for

the tar species. Validation is again performed against weight loss vs. pressure data such as those in Fig. 1, but the same criticism apply as in the previous section; there is a significant probability that the successful fit to the data is a result of parameter adjustability, since a non-softening coal model is being tested against softening coal data.

Gavalas and Wilks (13)

This model again applies only to non-softening coals. Its chemical structure is considerably less complicated than that of the previous two models:

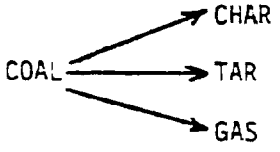

Note that no explicit account is taken of the competition between tar transport and repolymerization reactions. The volumetric generation rates of gas and tar are taken as constants (R_{gas} and R_{tar}). As a result, the model as presently cast cannot be used to predict the effect of pressure on total pyrolysis yield. The major emphasis in this model is placed on the proper accounting for porous matrix transport processes, and in this regard it is the most sophisticated of the three porous particle models discussed.

It is recognized that coal contains a highly crosslinked porous system, exhibiting a wide range of pore sizes. It is argued that the micropores are really too small to support true gas phase transport of any of the larger pyrolysis products (particularly tars). The transitional pores are treated as merely surface area for evolution of the volatiles from the bulk. Actual transport is considered only within the macropores. It is also concluded that a rather narrow range of macropore sizes embodies the majority of internal mass transfer resistance. These macropores are represented as having a diameter D_3, between 0.03 and 0.3 m. Larger macropores are claimed to represent minimal resistance to flow of volatiles, and thus are viewed as an extension of external particle boundary conditions to within the particle. A mathematical artifact is used to represent this assumption; an effective radius is defined for the particle. This effective radius is calculated based on assuming a fictitious particle which has just as many D_3 size pore mouths per unit volume on its periphery as the real particle has on both its periphery plus on macropores of diameter greater than D_3 within its interior. All solutions of the transport equations are based on this effective radius, rather than the true radius.

By virtue of the assumptions regarding the constancy of the source terms in Eq. 45, the direct integration results Eq. 46 apply in this case for both gases and tars. The r in Eq. 46 is now taken as the effective radius of the particle. The concentration profiles of various species within the particle are calculated from the total fluxes given in Eq. 46 by assuming a combined diffusion-convective flow of volatiles:

$$N_i = -(C_i B/\mu)dP/dr + N_{di} \qquad (55)$$

where B is the permeability, given by:

$$B = D_3^2 e_3/96 \qquad (56)$$

N_{di} is a pure diffusional flux, governed by:

$$\frac{dC_i}{dr} = \frac{N_{di}}{D_{ik}} + \sum_{j=1}^{3} \frac{y_i N_{dj} - y_j N_{di}}{D_{ij}} \qquad (57)$$

where D_{ik} is the Knudsen diffusivity of i, and the D_{ij} are the effective binary diffusion coefficients of i in j. Summing Eq. 57 for all species gives an expression for total gas phase concentration with position, which of course is equivalent to an expression for the pressure gradient in the particle. Used in conjunction with Eq. 55, this allows for simultaneous solution of the C_i as a function of position. Results of this model were presented only in this form, and no experimental validation was attempted.

A very interesting conclusion based on this model appears to be that the extent of pressure increase within the particle is quite small, for realistic values of the physical properties of coal. For example, a calculation for 89μm particles suggests that at atmospheric pressure conditions, the difference in pressure between the particle center and surface is less than 0.1 atm (for D_3 = 0.1μm). Such a low intraparticle pressure gradient would be consistent with the swelling model of Melia and Bowman (88) only if the viscosity of the coal to be used in Eq. 15 is fairly low (order 10^6 poise or less).

Apart from the predictions of pressure gradient and species concentration profiles, this model has not been used to make any other predictions of pyrolysis behavior. At the present time, it can be viewed only as a possible framework for further developments.

Simons (122-124)

This model is the same general class as those immediately preceding it. Again, it applies only to non-softening coals. A modified form of Eq. 45 is initially posed, assuming as usual pseudo-steady mass transport. This modified form of Eq. 45 is stated in terms of a rectangular coordinate y. The model postulates that the pore structures in coals are tree-like, and rules out "ink-bottle" structures. The coordinate y represents the straight line distance from the smallest pores in the tree towards the particle surface. The equivalent of Eq. 45 is then:

$$d/dy(n \rho_g C_g \pi r_p^2) = n \dot{m}_w \qquad (58)$$

where n is the number of pores in the tree at a particular position y, ρ_g and V_g are the volatiles density and velocity, respectively, r_p is the local pore radius at y, and $\dot{m}_w$ is a volatiles mass formation rate per unit length. A change of variables is effected by assuming a unique relation between r_p and y:

$$dr_p/dy = r_p/l_t \qquad (59)$$

where l_t is the "trunk" length of the largest pores (124). Integration is performed by introducing (see Ref. 123):

$$\dot{m}_w = \rho_s k \pi r_p^2 (e_f - e)/e \qquad (60)$$

where k is a pyrolysis rate constant and e_f is the final porosity of the char. The result obtained after assuming that V_g is zero in pores of the minimum size (r_{min}) and employing the ideal gas law is:

$$V_g = \frac{k l_t \rho_s R_g T}{P_g} \frac{(e_f - e)}{e} \ln (r_p/r_{min}) \qquad (61)$$

The actual volatiles flux (or velocity) is assumed to be governed by:

$$V_g = -D_v/\rho_g \, (d\rho_g/dy) \tag{62}$$

for Knudsen and continuum diffusional control, and by:

$$V_g = -sr_p^2(dP_g/dy) \tag{63}$$

for convective transport. For purely viscous drag, $s = 1/8\ \mu g$, while for the case in which the drag is due mainly to injection of large amounts of volatile into the flow $s = (\pi/\dot{m}_w)$. The four subcases of Eq. 62 and Eq. 63 are all considered individually, and after combination with Eq. 61, with a change of variables from y to r_p, are integrated piecewise over various regimes, in which the different mechanisms control. Boundary conditions for P_g are obtained by assuming that an arbitrary additive law governs P_g in the pore trunks: $P_{g,} = P_{tot} + P_{g,o}$, where P_{tot} is the ambient pressure and $P_{g,}$ is obtained by solving Eq. 61 for the case of V_g equal to the sonic velocity in the volatiles and r_p equal to the trunk radius. In addition, a limiting pressure is assumed to exist in the smallest pores, corresponding to the case in which the volatiles are formed but do not escape. This limit is calculated to be thousands of atmospheres in the case of non-softening coals which release very light volatiles. Actually, it is known that the molecular weight of volatiles generally shifts from high to low during the course of pyrolysis (H_2 is among the last products evolved). It is thus expected that maximum internal pressures would be achieved at some intermediate time during pyrolysis. Unfortunately, the present model does not yet include any variations with time, nor does it distinguish between different kinds of volatiles. As a result, comparison of this model with real experimental data is not yet possible.

Table of Nomenclature

a = constant

a_j = bubble radius (cm)

B = Permeability (cm^2)

C_v = vapor phase molar density ($moles/cm^3$)

C_L = liquid phase molar density ($moles/cm^3$)

C_i = molar density of species i ($moles/cm^3$) or in section 5.1.5 number concentration of bubbles of size i (cm^{-3})

C = a constant or in section 5.1.1, a non-dimensional volatiles concentration

D_L = liquid phase diffusivity (cm^2/s)

D_v = vapor phase diffusivity (cm^2/s)

D_{ij} = binary diffusion coefficient of i in j (cm^2/s)

D_{ik} = Knudsen diffusion coefficient of i (cm^2/s)

D_i = effective diffusion coefficient of i in a vapor mixture (cm^2/s)

D_{eff} = effective diffusion coefficient in pores (cm^2/s)

D_{micro}, D_{macro} = micro and macro-pore effective diffusion coefficients (cm^2/s)

D = pore diameter (cm)

e = void fraction

E = activation energy (kcal/mol)

E_i = number rate of escape of bubbles of size j from the particle surface (sec^{-1})

g = $k_1 C_v / k_o C_c$ (dimensionless)

K = $(1/e^2)-1$ in equation (10)

K = constant

K_m = mass transfer coefficient (sec^{-1})

K_j = bubble growth constant (sec^{-1})

k_{gi} = mass transfer coefficient for species i (cm/s)

k_o, k_1, k_2, k_i, k_r = reaction rate constants (sec^{-1})

k = overall pyrolysis rate constant (sec^{-1})

l_t = characteristic length of a pore "trunk" (cm)

L = characteristic length (cm)

m_i = mass of species i (g)

m = mass rate of volatiles evolution (g/s)

$\dot{m}_w$ = mass rate of volatiles evolution per length of pore (g/s cm)

M = moles of metaplast

MW = molecular weight (g/mol)

n = number of pores

N_i = molar flux of species i ($moles/cm^2 s$)

N_{io} = particle surface molar flux of species i ($moles/cm^2/s$)

P_b = bubble pressure (atm)

P_g = local gas pressure (atm)

P_{tot} = total pressure of atmosphere surrounding the particle (atm)

p^o, p_i^o = vapor pressure of tar (species i), (atm)

ΔP = pressure drop in a pore (atm)

P_{ij} = rate constant for merger of bubbles of size i and j (s^{-1})

q_i = D_{n+1}/D_i = ratio of inert gas diffusivity to species i diffusivity

Q_r = mass formation rate of reactive volatiles per unit mass of coal (s^{-1})

Q_L = rate of formation of volatiles in coal melt ($moles/cm^3 s$)

r = pore radius or general radial position in a particle (cm)

R, R_p = particle radius (cm)

R_g = gas constant (= 1.987 cal/mol K)

R_i = production rate of species i per unit volume ($moles/cm^3 s$)

s = constant defined below equation (43)

t, t_i = time (s)

T = temperature (K)

T_b = boiling temperature (K)

u = $(1 - \sum_{i=1}^{n} y_{io})^{-1}$ (dimensionless)

v = volatiles mass yield (g)

v_o = volatiles mass yield at vacuum conditions (g)

v_h = volatiles mass yield at high pressure (g)

V_r = fractional mass yield of reactive volatiles (dimensionless)

V_{nr} = fractional mass yield of non-reactive volatiles (dimensionless)

v_m = specific volume of metaplast (cm^3/g)

V_b = bubble velocity (cm/s)

V_g = gas velocity (cm/s)

w_b = shortest distance from bubble to particle surface (cm)

x = distance for a species to diffuse to a pore (cm)

x_i = mole fraction of i in the liquid phase

y_i = vapor phase mole fraction of species i

y_{io} = vapor phase mole fraction of i at the particle surface

y = distance from smallest pore to particle surface (cm)

Greek

δ_m = diffusion film thickness (cm)

μ = viscosity (g/s-cm)

μ' = dimensionless viscosity

ρ = true mass density of liquid (g/cm_3)

ρ_g = local volatiles density (g/cm^3)

ρ_s = true solids density (g/cm^3)

σ = surface tension (dyne/cm)

REFERENCES

1. Suuberg, E.M., in Chemistry of Coal Conversion, (R.H. Schlosberg, Ed)., Chapter 4, Plenum Press, NY, (1985).

2. Anthony, D.B. and Howard, J.B., AIChE Journal, **22**, 625, (1976).

3. Howard, J.B. in Chemistry of Coal Utilization, Second Supplementary Vol., (M. Elliott, Ed). pp 625-784, Wiley 1981.

4. Gavalas, G.R., Coal Pyrolysis, Elsevier, (1982).

5. Suuberg, E.M., Peters, W.A., and Howard, J.B., in Thermal Hydrocarbon Chemistry, (A. Oblad et al., Eds.), ACS Advances in Chemistry Series, No. 183, Chap. 14, (1979).

6. Suuberg, E.M., Peters, W.A., and Howard, J.B., 17th Symp. (Int) on Combustion, The Combustion Institute, Pittsburgh, PA, pg. 117, (1979).

7. Suuberg, E.M. and Unger, P.E., Fuel, **63**, 606, (1984).

8. Niksa, S., Russel, W.B., and Saville, D.B., 19th Symp. (Int) on Combustion, The Combustion Institute, Pittsburgh, PA, pg. 1151, (1982).

9. Suuberg, E.M., Peters, W.A., and Howard, J.B., Ind. Eng. Chem. Proc. Des. Dev. **17**, 37 (1978).

10. Solomon, P.R. and Colket, M.B., 17th Symp. (Int) on Combustion, The Combustion Institute, Pittsburgh, PA, pg. 131, (1979).

11. Seeker, W.R., Samuelson, G.S., Heap, M.F., and Trolinger, J.D., 18th Symp. (Int) on Combustion, The Combustion Institute, Pittsburgh, PA, pg. 1213, (1981).

12. Mclean, W.J., Hardesty, D.R., and Pohl, J.H., 18th Symp. (Int) on Combustion, The Combustion Institute, Pittsburgh, PA, pg. 1239, (1981).

13. Gavalas, G.R. and Wilks, K.A., AIChE, **26**, 201, (1980).

14. Arendt, P. and van Heek, K.H., Fuel, **60**, 779, (1981).

15. Unger, P.E. and Suuberg, E.M., Proc. of the 1983 Int. Conf. on Coal Science, pg. 475, Int. Energy Agency, (1983).

16. Howard, H.C., in Chem. of Coal Utilization, (H.H. Lowry, Ed), pg. 761ff, John Wiley, (1945).

17. Anthony, D.B., Howard, J.B., Hottel, H.C., and Meissner, H.P., 15th Symp. (Int) on Combustion, The Combustion Institute, Pittsburgh, PA, pg. 1303, (1974).

18. Howard, J.B., Peters, W.A., and Serio, M.A., EPRI Report Ap-1803, Electric Power Research Institute, Palo Alto, CA (April, 1981).

19. Parks, B.C., in Chem. of Coal Util. Suppl. Vol., (H.H. Lowry, Ed.), p.1ff, John Wiley, NY, (1963).

20. Howard, H.C., in Chem. of Coal Util. Suppl. Vol., (H.H. Lowry, Ed.), p.340ff, John Wiley, NY, (1963).

21. Orning, A.A. and Greifer, B., Fuel, 35, 381, (1956).

22. Brown, J.K., Dryden, I.G.C., Dunevein, D.H., Joy, W.K., and Pankhurst, K.S., J. Inst. Fuel, 31, 259, (1958).

23. Solomon, P.R. and Colket, M.B., Fuel, 57, 749, (1978).

24. Unger, P.E. and Suuberg, E.M., ACS Div. of Fuel Chem. Preprints, 28, (4), 278, (1983).

25. Unger, P.E. and Suuberg, E.M., 18th Symp. (Int) on Combustion, The Combustion Institute, Pittsburgh, PA, pg. 1203, (1981).

26. Williams, F.A., Combustion Theory, Addison-Wesley, p.47ff, (1965).

27. Newbold, F.R. and Amundson, N.R., AIChE, 19, 22, (1973).

28. Law, C.K., Prakash, S., and Sirignano, W.A., 16th Symp. (Int) on Combustion, The Combustion Institute, Pittsburgh, PA, pg. 605, (1977).

29. Law, C.K., Prog. Energy Comb. Sci., 8, 171, (1982).

30. Johnson, J.L., in Chem. of Coal Util. Second Suppl. Vol., (M.A. Elliott, Ed.), p1498ff, John Wiley, NY (1981).

31. Mahajan, O.P., Tomita, A., Nelson, J.R., and Walker, P.L., Jr., ACS Div. of Fuel Chem. Preprints, 20, (3), 19, (1975).

32. Merrick, D., Fuel, 62, 540, (1983).

33. Suuberg, E.M., Unger, P.E., and Lilly, W.D., Fuel, 64, 956, (1985).

34. Solomon, P.R., Squire, K.R., and Carangelo, R.M., Proc. of the 1985 Int. Conf. on Coal Sci., pg. 945, Pergamon Press, (1985).

35. Solomon, P.R., and King, H.H., Fuel, 63, 1302, (1984).

36. Solomon, P.R., and Squire, K.R., ACS Div. of Fuel Chem. Preprints, 30, (4), 346, (1985).

37. Anbar, M. and St. John, G.A., Fuel, 57, 105, (1978).

38. Suuberg, E.M., Unger, P.E., and Larsen, J.W., Energy and Fuels, in Press.

39. Unger, P.E., Ph.D. Thesis, Dept. of Chemical Engineering, Carnegie-Mellon University, Pittsburgh, PA, (1983).

40. Solomon, P.R., Squire, K.R., and Carangelo, R.M., ACS Div. of Fuel Chem. Preprints, 29, (1), 10, (1984).

41. Fuller, E.N., Schettler, P.D., and Giddings, J.C., Ind. Eng. Chem. 58, 19, (1966).

42. Zacharias, M.W., S.M. Thesis, Dept. of Chem. Eng., MIT, (Advisor: J.B. Howard), (1979).

43. Berkowitz, N., An Introduction to Coal Technology, Academic PRess, pg. 87ff, (1979).

44. Loison, P., Peytavy, A., Boyer, A.F., and Grillot, R., in Chemistry of Coal Util. Suppl. Vol., (H.H. Lowry, Ed.), p150ff, John Wiley, NY, (1963).

45. van Krevelen, D.W., Coal, p 452ff and p271ff, Elsevier, (1961).

46. Habermehl, D., Crywal, F., and Beyer, H.D., in Chem. of Coal Util. Second Suppl. Vol., (M.A. Elliott, Ed.), p317ff, John Wiley, NY, (1981).

47. Neavel, R.C. in Coal Science, Vol. 1, (M. Gorbaty, et al., Eds.), p1 Academic Press, NY, (1982).

48. Solomon, P.R., Serio, M.A., Carangelo, R.M., and Markham, J.R., Fuel, **65**, 182, (1986).

49. Hamilton, L., Fuel, **60**, 909, (1981).

50. Wolfs, P.M.J., van Krevelen, D.W., and Waterman, H.I., Fuel, **39**, 25, (1960).

51. Fitzgerald, D., Nature, **175**, 515, (1955).

52. Fong, W.S., Peters, W.A., and Howard, J.B., Fuel, **65**, 251, (1986).

53. Fong, W.S., Sc.D. Thesis, Department of Chemical Engineering, MIT, (1986)

54. Lara-Urbaneja, P. and Sirignano, W.A., 18th Symp. (Int) on Combustion, The Combustion Institute, Pittsburgh, PA, p1365, (1981).

55. Attar, A., AIChE, **24**, 105, (1978).

56. Lewellen, P.C., S.M. Thesis, Department of Chemical Engineering, MIT, (1975).

57. Karl, F.S., Friedel, R.A., Thames, B.M., and Sharkey, A.G., Jr., Fuel, **49**, 249, (1970).

58. Nandi, S.P. and Walker, P.L., Jr., Fuel, **49**, 309, (1970).

59. Thimons, E.D. and Kissell, Fuel, **52**, 50, (1973).

60. Walker, P.L., Jr. and Mahajan, O.P., in Analytical Methods for Coals and Coal Products, Vol. I, (C. Karr, Ed.), p163ff, Academic Press, (1978).

61. Nandi, S.P. and Walker, P.L., Jr., in Coal Science, (P.H. Given, Vol. Ed), Advances in Chem. Ser. No. 55, p 379, (1966).

62. Lee, M., Guin, J.A., and Tarrer, A., Ind. Eng. Chem. Proc. Des. Dev., **17**, 127, (1979).

63. Hiss, T.G. and Cussler, E.L., AIChE, **19**, 698, (1973).

64. Riazi, M.R. and Daubert, T.E., AIChE, **26**, 386, (1980).

65. Hershkowitz, F., in Chemistry of Coal Conversion, (R. Schlosberg, Ed.), Chapter 3, Plenum Press, NY, (1985).

66. Baltus, R.E. and Anderson, J.L., Chem. Eng. Sci. **38**, 1959, (1983).

67. Essenhigh, R.H., in Chem. of Coal Util. Second Suppl. Vol., (M.A. Elliott, Ed.), p1188ff, John Wiley, NY, (1981).

68. Littlejohn, R.F., J. Inst. Fuel, 40, 128, (1967).

69. Street, P.J., Weight, R.P., and Lightman, R., Fuel, 48, 343, (1969).

70. Solomon, P.R., Hamblen, D.G., Carangelo, R.M., and Krause, J.L., 19th Symp. (Int) on Combustion, The Combustion Institute, Pittsburgh, PA, p1139, (1982).

71. Simmott, F.S., McCulloch, A., and Newall, H.E., JSCI Transactions, 46, 331(T), (1927).

72. Alpern, B., Courbon, P., Plateau, J., and Tissandier, G., J. Inst. Fuel, 33, 399, (1960).

73. Shibaoka, M., J. Inst. Fuel, 42, 59, (1969).

74. Lightman, P., Street, P.J., and Weight, R.P., J. Inst. Fuel, 40, 433, (1967).

75. Matsunaga, T., Nishiyama, Y., Sawabe, H., and Tamai, U., Fuel, 57, 562, (1978).

76. Dolan, J.F., Sc.B. Thesis, Chemical Engineering Department, MIT, (1980).

77. Green, P.D. and Thomas, K.M., Fuel, 64, 1423, (1985).

78. Khan, M.R. and Jenkins, R.G., Fuel, 64, 189, (1985), and 63, 109, (1984).

79. Pohl, J.E., Sc.D., Thesis, Department of Chemical Engineering, MIT, (1976).

80. Rowe, P.N., Claxton, K.T., and Lewis, J.B., Trans. Inst. Chem. Eng., 43, T14-T31, (1965).

81. Smoot, L.D. and Pratt, D.T., Editors, Pulverized Coal Combustion and Gasification, Plenum Press, NY, (1979).

82. Smoot, L.A. and Smith, P.J., Coal Combustion and Gasification, Plenum Press, NY, (1985).

83. Field, M.A., Gill, D.W., Morgan, B.B., And Hawksley, P.G.W., BCURA Monogr. Bull. 31, 285, (1967).

84. Russel, W.B., Saville, D.A., and Greene, M.I., AIChE J., 25, 65, (1979).

85. Chen, L.W. and Wen, C.Y., ACS Div. of Fuel Chem. Preprints, 24, (3), p141, (1979).

86. Mills, A.F., James, R.K., and Antoniuk, D., "Analysis of Coal Particles Undergoing Rapid Pyrolysis", Int. Center for Heat and Mass Transfer, International Seminar, Dubrovnik, (Aug. 1975).

87. James, R.K. and Mills, A.F., Letters in Heat and Mass Transfer, 3, 1, (1976).

88. Melia, P.F. and Bowman, C.T., Comb. Sci. and Tech. 31, 195, (1983), and "An Analytical Model for Coal Particle Pyrolysis and Swelling", paper presented at the Western States Section of the Combustion Institute, Salt Lake City, (April, 1982).

89. Oh, M.S., Howard, J.B., and Peters, W.A., "Modeling Volatiles Transport in Softening Coal Pyrolysis", paper presented at the San Francisco Meeting of the AIChE, (Nov. 1984).

90. Oh, M., Peters, W.A., and Howard, J.B., Proc. of the 1983 Int. Conf. on Coal Sci., p 483, International Energy Agency, (1983).

91. OH, M.S., Sc.D. Thesis, Department of Chemical Engineering, MIT (1985).

92. Pelofsky A.H., J. Chem. Eng. Data, 11, (3), 394, (1966).

93. Hwang, S.C., Tsonopoulos, L., Cunningham, J.R., and Wilson, G.W., I.E.C. P.D.D. 21, 127, (1982).

94. Serio, M.A., Ph.D. Thesis, Department of Chemical Engineering, MIT, (1984).

95. Bronowski, J., Fitzgerald, D., Gillings, D.W., Phys-Jones, D.C., Nature, 171, 389, (1953).

96. Bird, R.B., Stewart, W.E., and Lightfoot, E.N., Transport Phenomena, p570ff, John Wiley, NY, (1960).

97. Suuberg, E.M. and Sezen, Y., Proc. of the 1985 Int. Conf. on Coal Sci., p913, Pergamon Press, (1985).

98. Solomon, P.R. and Hamblen, D.G., in Chemistry of Coal Conversion, (R.H. Schlosberg, Ed.), Chap. 5, Plenum Press, NY, (1985).

99. Solomon, P.R. and Hamblen, D.G., Prog. Energy Comb. Sci., 9, 323, (1983).

100. Hanbaba, P., Juntgen, H., and Peters, W., Brennst.-Chem., 49, 368, (1968).

101. Juntgen, H. and van Heek, K.H., Fortschr. der Chem. Forsch., 13, 601, (1970).

102. Juntgen, H. and van Heek, K.H., Fuel Proc. Tech., 2, 261, (1979).

103. Weimer, R.F. and Ngan, D.Y., ACS Div. of Fuel Chem. Preprints, 24, (3), 129, (1979).

104. Campbell, J.H., Gallegos, G., and Gregg, M., Fuel, 59, 727, (1980).

105. Green, T., Kovac, J., Brenner, D., and Larsen, J.W., in Coal Structure, (R. Meyers, Ed.), Chapter 6, Academic Press, (1982).

106. Gavalas, F.R., Cheong, P.H., and Jain, R., IEC Fund. 20, 113 and 122, (1981).

107. Solomon, P.R., Hobbs, R.H., Hamblen, D.G., Chen, W., LaCava, A., and Graff, R.S., Fuel, 60, 342, (1981).

108. Mahajan, O.P. and Walker, P.L., Jr., in Analytical Methods for Coal and Coal Products, Vol. I, (C. Karr, Ed.), p125ff, Academic Press, (1978).

109. Mahajan, O.P., in Coal Structure, (R. Meyers, Ed.), Chapter 3, Academic Press, (1982).

110. Grimes, W.R., in Coal Science, Vol. 1, (M. Gorbaty, et al., Eds.), p 21, Academic Press, (1982).

111. Gan, H., Nandi, S.P., and Walker, P.L., Jr., 51, 22, (1972).

112. Toda, Y., Fuel, 52, 36, (1973).

113. Franklin, R., Trans. Faraday Soc., 45, 668, (1949).

114. Tschamler, H. and DeRuiter, E., in Chem. of Coal Util. Suppl. vol., (H.H. Lowry, Ed.), p35ff, John Wiley, NY (1963).

115. Nsakala, N., Essenhigh, R.H., and Walker, P.L., Jr., ACS Div. of Fuel Chem Preprints, 22, (1), 1012, (1977).

116. Anson, D., Moles, F.D., and Street, P.J., Comb. and Flame, 16, 265, (1971).

117. Jiang, W.D., Lee, I.C., and Yang, R.Y.K., ACS Div of Fuel Chem. Preprints, 32, (1), 247, (1987).

118. Jenkins, R.G., Nandi, S.P., and Walker, P.L., Jr., Fuel, 52, 288, (1973).

119. Walker, P.L., Jr., Fuel, 59, 809, (1980).

120. Russel, W.B., Saville, D.A., and Greene, M.I., AIChE J., 25, 65, (1979).

121. Chen, L.W. and Wen, C.Y., ACS Div. of Fuel Chem. Preprints, 24, (3), 141, (1979).

122. Simons, G., Comb. and Flame, 53, 83, (1983).

123. Simons, G., Comb. and Flame, 55, 181, (1984).

124. Simons, G., 19th Symp. (Int). on Combustion, The Combustion Institute, Pittsburgh, PA, pg 1067, (1982).